

A Survey on Prototype Filter Design for Filter Bank Based Multicarrier Communications

Alphan Şahin¹, İsmail Güvenç², and Hüseyin Arslan¹

¹Department of Electrical Engineering, University of South Florida, Tampa, FL, 33620

²DOCOMO Innovations, Inc., 3240 Hillview Avenue, Palo Alto, CA, 94304

Email: alphan@mail.usf.edu, iguvencc@ieee.org, arslan@usf.edu

Abstract—Due to its numerous advantages, orthogonal frequency division multiplexing (OFDM) has been the broadband wireless access technology of choice for many wireless standards over the last decade. Recently, filter bank based multicarrier techniques are emerging as one of the alternatives to OFDM for next generation broadband wireless access systems. While there are several studies on filter bank based multicarrier systems in the literature, its potential merits over OFDM and possible implementation challenges in practical channel and impairment conditions require further investigations. The goals of the present survey are to provide an extensive and unified review of waveform design issues for filter bank based multicarrier systems, shed some light on advantages and disadvantages of this technology, and provide pointers to open research problems.

Index Terms—biorthogonal modulation, filter-bank multicarrier (FBMC), future radio access, hermite pulse, IOTA, OFDMA, BFD, PHYDYAS filter, polyphase network (PPN), pulse shaping, waveform design

I. INTRODUCTION

Increasing number of users, wide variety of wireless communication applications, and extensive growth of the user demands from the wireless communication systems lead more adaptive, flexible and efficient future radio access techniques. Over last decade, orthogonal frequency division multiplexing (OFDM) has been the radio access technology of choice for many wireless standards, such as 802.11a/b/g under WiFi alliance, 802.16 (WiMax), DVB-T/DAB-T, WRAN 802.22, and Long Term Evolution (LTE) of cellular radio. Some advantages of OFDM include simple equalization in frequency domain, less complex implementations through fast Fourier transformation (FFT), efficient usage of spectrum through frequency overlapping while limiting time signal over a perfect rectangular block, and suitability for multiple-input multiple-output (MIMO) systems. In addition, possibility to exploit multiuser diversity and frequency diversity make OFDM an appealing technology for many wireless systems. On the other hand, new waveform design for the next-generation broadband wireless access (BWA) systems carries critical importance due to shortcomings of OFDM such as high sidelobes, susceptibility to carrier frequency offset (CFO) and doubly dispersive channels, cyclic prefix (CP) overhead, and larger peak-to-average-power ratio (PAPR).

Filter bank multicarrier (FBMC) is one of the BWA options that may address the shortcomings of OFDM while maintaining some of its advantages. Earlier works related to FBMC actually date back to 1960s [1], [2], which utilize a bank of

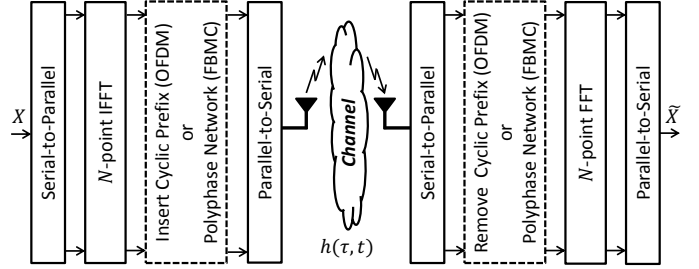


Fig. 1: Transmitter and receiver block diagrams in OFDM and FBMC.

filters for parallel data transmission. In [1], Chang presented the orthogonality condition for the multicarrier transmission schemes considering band-limited filters and offset quadrature amplitude modulation (OQAM). This condition basically indicates that the subchannels can be spaced half of the symbol rate apart without any inter-carrier interference (ICI) and inter-symbol interference (ISI) when the data is staggered on alternate in-phase and quadrature subchannels. This multicarrier transmission idea has then been generalized by Saltzberg in 1967 [2] by showing the fact that Chang's condition is also true when the time and frequency axes are interchanged. However, the idea of parallel transmission suggested in [1] and [2] required *unreasonably expensive and complex* for large number of data channels at that time. In [3], through the use of discrete Fourier transformations (DFTs), Weinstein and Ebert eliminated the banks of subcarrier oscillators and allow simpler implementation of the multicarrier schemes. This approach has been later named as OFDM, and it has become more and more popular after 1980s due to its efficient implementation through FFT techniques and frequency domain equalization (FDE) along with CP utilization [4] compared to FBMC approaches¹. On the other hand, Weinstein's DFT method in [3] limits the flexibility on different baseband filter utilization while modulating or demodulating the subcarriers, but instead used a time windowing technique to cope with the ICI. In [5], by extending Weinstein's method, Hirotsaki showed that the

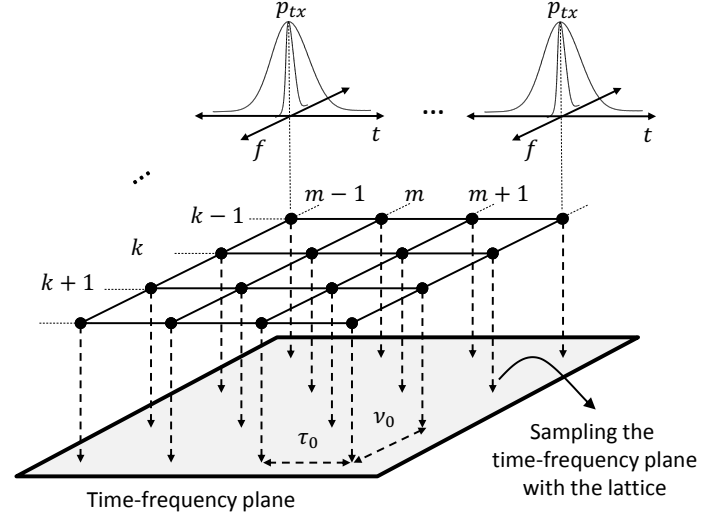
¹In the literature, the phrase of *orthogonal frequency division multiplexing* is conventionally used for the scheme that is based on rectangular filters. However, FBMC approaches with other filters can also satisfy the orthogonality conditions. Indeed, the phrase of *orthogonal frequency division multiplexing* embraces the FBMC scheme.

different baseband filter may also be digitally implemented through DFT processing by using a poly phase network (PPN) [6], [7]. As shown in Fig. 1, transmitter/receiver block diagrams of OFDM and FBMC are very similar to each other. At the transmitter, inverse fast Fourier transformation (IFFT) operation is followed by CP insertion in OFDM (to combat with ISI), while it is followed by a PPN in FBMC. In the same manner, CP removal is substituted with PPN in FBMC to extract the information symbols at the receiver. Several other developments over the last two decades have demonstrated low complexity and efficient implementations of FBMC, paving the way for its consideration in the next generation wireless standards (see e.g., [8]–[11], and the references listed therein).

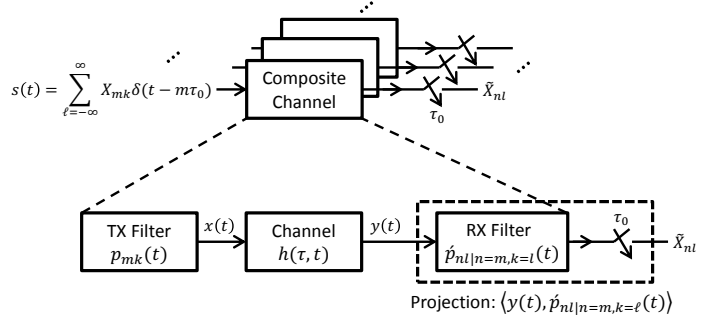
In the literature, two main advantages of FBMC compared to the conventional OFDM are emphasized. First, FBMC may use any prototype filter design (captured through the PPN). By applying different filter coefficients to PPN structure, it is possible to yield better adaptations to channel characteristics and other design constraints without changing the implementation. Secondly, FBMC exploits the sparser structure of time-frequency grid compared to the conventional OFDM. Therefore, it *allows* the use of better-localized prototype filters in both time and frequency domains. For example, the lattice grid with staggered modulations in FBMC *effectively* halve the density of the lattice with quadrature amplitude modulation (QAM) [11], [12]. Therefore, FBMC provides a way to improve the ISI/ICI performances of the systems in doubly dispersive channel with the proper filter selections. In the literature, this interference immunity is exploited to remove the guard time between symbols, which yields more spectral efficient schemes compared to OFDM. Beside these well-known advantages, if the concept of biorthogonality, i.e., different prototype filters at the transmitter and receiver, is included to FBMC, it is also possible to show the impact of prototype filters to equalization domain. For example, CP-OFDM offers FDE by using inherently unsymmetrical utilization of the filters, i.e., rectangular filter at the receiver and the *extended* rectangular pulse at the transmitter, which obeys to the nature of biorthogonality [13], [14]. With this perspective, a generic framework to study different waveforms including OFDM and equalization approaches can be constructed in the sense of different configurations of the filters.

With the recent developments in filter bank based approaches and the urge to improve next generation wireless access capacity and flexibility dictated by the wireless traffic trends [15], filter bank based multicarrier systems emerges as an umbrella for the transmission schemes, and promises to be an alternative radio access technology. The goal of this survey paper is to provide an extensive and unified review of waveform design issues for filter bank based multicarrier systems. Pointing open research problems on FBMC also constitutes another major aim of this survey paper by shedding some light on advantages and disadvantages of the filters.

The paper is organized as follows: The classification of multicarrier systems is provided considering both orthogonal and biorthogonal Gabor systems in Section II. Then, well-known prototype filters in the literature are represented mathematically and the trade-offs between these filters are



(a) Gabor system at the transmitter. Prototype filter is employed in time-frequency plane at different locations considering the lattice at the transmitter to construct the transmitted signal. The product of $\nu_0 \tau_0$ corresponds to the sampling density of the lattice. Another Gabor system is also constructed at the receiver to recover the information symbols.



(b) Considering parallel transmission, projection of the received signal on to the analysis function corresponds to getting sample after received filter every other τ_0 and ν_0 .

Fig. 2: Utilizing the prototype filters at the transmitter and the receiver sides in time and frequency domains in FBMC based systems.

explained in Section III. Useful tools and metrics to evaluate the filter performances are investigated in Section IV. Then, the comparison of the filters are provided in view of time-frequency characteristics, sidelobe performance, signal-to-interference ratio (SIR) performance in wireless channels and truncation in Section V. Considering all of these investigation on filters, transceiver design issues on FBMC are investigated from different perspectives in Section VI. Finally, the paper is concluded in Section VII.

II. MULTICARRIER COMMUNICATIONS

In a multicarrier transmission, the information symbols are transmitted over the points of a lattice as follows [16], [17]

$$p_{mk}(t) = p_{tx}(t - m\tau_0) e^{j2\pi k\nu_0 t}, \quad (1)$$

where $p_{tx}(t)$ is the prototype filter, ν_0 is the subcarrier spacing, τ_0 is the symbol spacing, m is the symbol index, and k is the subcarrier index. The family of functions in (1) is often

referred to as a *Gabor system*, and $p_{mk}(t)$ is called in various names like *synthesis function*, *window*, *atom*, or *pulse shape* which maps information symbols into time-frequency plane considering a lattice grid for different m and k as in Fig. 2(a) [18]. Therefore, considering N subchannels, the transmitted signal in the baseband is given by [12], [19]

$$x(t) = \sum_{m=-\infty}^{\infty} \sum_{k=0}^{N-1} X_{mk} p_{mk}(t), \quad (2)$$

where X_{mk} is the complex or real information symbol transmitted at the grid point (m, k) . Then, the spectral efficiency of this system can be written as [19], [20]

$$\eta = \frac{\beta}{\tau_0 \nu_0} \text{ [bits/sec/Hz]}, \quad (3)$$

where β is the number of bits per symbol.

After the transmitted signal given in (2) passes through the linear time-varying wireless channel $h(\tau, t)$, the received signal is obtained as

$$\begin{aligned} y(t) &= \int_{\tau} h(\tau, t) x(t - \tau) d\tau + w(t) \\ &= \int_{\tau} \int_{\nu} H(\tau, \nu) x(t - \tau) e^{j2\pi\nu t} d\nu d\tau + w(t), \end{aligned} \quad (4)$$

where $H(\tau, \nu)$ is the Fourier transform of $h(\tau, t)$ and $w(t)$ is the additive white Gaussian noise (AWGN). Therefore, as indicated in Fig. 2(b), the received symbol \tilde{X}_{nl} located on time index n and frequency index l is obtained by the projection of the received signal on to analysis function $\dot{p}_{nl}(t)$ as

$$\begin{aligned} \tilde{X}_{nl} &= \langle y(t), \dot{p}_{nl}(t) \rangle \triangleq \int_t y(t) \dot{p}_{nl}^*(t) dt \\ &= X_{nl} H_{nl} + \sum_{(m,k) \neq (n,l)} X_{mk} H_{nlmk} + w_{nl}, \end{aligned} \quad (5)$$

where

$$\dot{p}_{nl}(t) = p_{rx}(t - n\tau_0) e^{j2\pi l \nu_0 t} \quad (6)$$

is the receiver filter offset in time by $n\tau_0$ and in frequency by $l\nu_0$, w_{nl} is the noise after projection, and

$$H_{nlmk} = \int_{\tau} \int_{\nu} H(\tau, \nu) \int_t p_{mk}(t - \tau) \dot{p}_{nl}^*(t) e^{j2\pi\nu t} dt d\nu d\tau \quad (7)$$

captures the interference from the symbol (m, k) to the desired symbol (n, l) . Similar to (2), $\dot{p}_{nl}(t)$ given in (6) is obtained by another prototype filter $p_{rx}(t)$ shifted in both time and frequency domains depending on (n, l) . In other words, both $p_{mk}(t)$ and $\dot{p}_{nl}(t)$ denote banks of filters based on Gabor system at the transmitter and receiver sides.

A. Reconstruction and Representation in Gabor Systems

The time-frequency characteristics of $p_{tx}(t)$ and $p_{rx}(t)$ employed in the scheme, and the lattice structure identified by τ_0 and ν_0 are related with the representation and the reconstruction properties of FBMC based transmissions. These properties can be investigated via Gabor analysis. In Gabor analysis, the product of $\nu_0 \tau_0$ indicates the density of the

sampling lattice as in Fig. 2(a). It determines not only the spectral efficiency of the transmission as in (3), but also the representability of the signal space, and the invertibility of the transformation between information symbols and constructed signal in (2) under AWGN or ideal channels. Basically, the perfect reconstruction of a signal compels to use *linearly independent* set of $p_{mk}(t)$, since this property corresponds to invertibility of a transformation. On the other hand, the representability of the Hilbert space $\mathcal{L}^2(\mathbb{R})$ of square-integrable functions with the set of $p_{mk}(t)$ is equivalent to the *completeness* property of the Gabor system. While including an extra basis function to the basis spoils the *linear independency*, discarding a basis function from the space destroys the *completeness* of the system. However, it is important to note that whereas linear independence is conservative condition for the communication systems, *completeness* is not that important [22]. As an extension of the concept of a basis, *Frames*, introduced in 1952 by Duffin and Schaeffer [23], might not be linearly independent. In other word, a frame might include more than the required functions to span a space. This issue yields to an *overcomplete* systems, which might cause lossy reconstruction [24], [25]. Considering the spectral efficiency, *linear independency* and *completeness* of the systems, FBMC-based systems are classified for an ideal channel regarding to the product of $\nu_0 \tau_0$ in TABLE I and described as follows [16], [18]:

- Undersampled grid ($\nu_0 \tau_0 > 1$): In this case, Gabor system given in (1) cannot be a complete basis or a frame since the lattice is not sampled sufficiently. However, it still allows linear independency between the basis functions. Therefore, well-localized prototype filters obtained from incomplete bases can be adapted to the communication systems. However, the spectral efficiency of the system degrades with increasing $\nu_0 \tau_0$ product when the complex information symbols are utilized. On the other hand, transmitting in-phase and quadrature components in staggered manner, e.g., OQAM, the spectral efficiency can be still maintained as $\nu_0 \tau_0 = 1$. Also, this approach yields an undersampled grid structure where $\nu_0 \tau_0 = 2$.
- Critically sampled grid ($\nu_0 \tau_0 = 1$): It results in a complete Gabor System. Orthogonal bases exist, but according to the Balian-Low theorem [26], critically sampled grid cannot utilize well-localized prototype filters, and instead, dictates the filter with bad time-frequency localization, e.g., rectangular filter. The spectral efficiency is maximized for $\tau_0 \nu_0 = 1$, since the perfect reconstruction might not be possible beyond the critically sampled grid condition [16]. Pure OFDM symbols, which does not to use CP or zero padding (ZP), is constructed with critically sampled grid. However, employing CP or ZP leads a system with undersampled grid because of the coarsification of the lattice in time domain.
- Oversampled grid ($\nu_0 \tau_0 < 1$): In this case, an overcomplete set of functions is obtained. Gabor system cannot be a basis, but it might be a frame with well-localized pulse shape. However, since the Gabor system is overcomplete, in a perfect channel, representation of a signal might not

Perfect Reconstruction		Conditional Perfect Reconstruction
$\nu_0\tau_0 > 1$ (e.g. SMT, CMT, FMT, CP/ZP-OFDM)	$\nu_0\tau_0 = 1$ (e.g. pure OFDM)	$\nu_0\tau_0 < 1$
Linear Independent Systems (Bases)		Linear Dependent Systems (Frames)
Incomplete Systems for $\mathcal{L}^2(\mathbb{R})$	Complete Systems for $\mathcal{L}^2(\mathbb{R})$	Overcomplete Systems for $\mathcal{L}^2(\mathbb{R})$
Orthonormal Systems (e.g. pure OFDM, ZP-OFDM, SMT, CMT, FMT)		
$X_{nl} = \left\langle \sum_{mk} X_{mk} p_{mk}, \dot{p}_{nl} \right\rangle$ and $\dot{p}_{mk} = p_{mk}$		
Biorthogonal Systems (e.g. CP-OFDM)		
$X_{nl} = \left\langle \sum_{mk} X_{mk} p_{mk}, \dot{p}_{nl} \right\rangle = \left\langle \sum_{mk} X_{mk} \dot{p}_{mk}, p_{nl} \right\rangle$ and $\dot{p}_{mk} \neq p_{mk}$		

TABLE I: Classification of FBMC-based schemes respect to the product of $\nu_0\tau_0$ in Gabor systems. Selecting $\nu_0\tau_0 \geq 1$ allows linear independent bases which are crucial for the communication systems. While the orthogonal systems dictate to use the same set of functions at the transmitter and receiver, biorthogonal system allows to use different Gabor systems at the receiver and the transmitter with the perfect reconstruction property. Employing different Gabor systems at the transmitter and receiver introduces a flexibility on selecting the basis to combat with the doubly dispersive channels. On the other hand, the reconstruction of information symbols perfectly in Gabor systems is conditionally possible when $\nu_0\tau_0 < 1$ because of including more than required number of basis functions. For example, employing finite-alphabet for the transmitted information symbols can allow a system where $\nu_0\tau_0 < 1$ with the perfect reconstruction property [21].

be unique. Therefore, the reconstruction might be lossy [18], [19].

When $\nu_0\tau_0 < 1$, specific conditions might yield the perfect symbol reconstruction. This issue firstly is investigated by Mazo in 1974 as faster-than Nyquist (FTN) by addressing the following question: what extend can be the symbols packed more than the Nyquist rate without loss in bit error rate (BER) performance? It is shown that the symbol spacing can be reduced to $0.802T$ without suffering any loss in minimum Euclidean distance for binary information symbols and sinc pulse [27]. In other words, ISI-free BER performance is still achievable with the optimal maximum a posteriori (MAP) sequence detector even when the symbols are transmitted at a rate greater than Nyquist rate. The minimum symbol spacing that keeps the minimum Euclidean distance is later on called *Mazo limit*. By generalizing FTN approach to other pulses, various Mazo limits are obtained for root-raised cosine (RRC) pulses with different roll-off factors in [28]. For example, when roll-off is set to 0, 0.1, 0.2, and, 0.3, Mazo limits are derived as 0.802, 0.779, 0.738, and, 0.703 respectively. The FTN approach is extended to multicarrier schemes by allowing both ICI and ISI in [29], [30]. It is shown that two dimensional signaling is more bandwidth efficient than one dimensional. Another way of developing a scheme where $\nu_0\tau_0 < 1$ is to transmit correlated symbols. This approach corresponds to partial-response signaling (PRS) and introduced in [31]. Similarly, employing finite-alphabet for the transmitted information symbols along with frames can allow a system where $\nu_0\tau_0 < 1$ with the perfect reconstruction property [21].

In this survey, we consider only *complete* and *incomplete* linear independent systems, i.e. $\nu_0\tau_0 \geq 1$, to discuss the schemes allowing the practical communication systems.

B. Orthogonal and Biorthogonal Systems

For the sake of clarity, if the channel is assumed ideal and the noise is ignored in (5), the information symbols are obtained by

$$X_{nl} = \underbrace{\left\langle \sum_{mk} \overbrace{X_{mk} p_{mk}(t), \dot{p}_{nl}(t)}^{\text{Transmitted signal}} \right\rangle}_{\text{Received symbol}}. \quad (8)$$

In finite dimensional vector space, this operation corresponds to

$$X_{mk} = \underbrace{T \overbrace{T^{-1} X_{mk}}^{\text{Transmitted signal}}}_{\text{Received symbol}} \quad (9)$$

where

$$T = \begin{bmatrix} - & \dot{p}_{0,0}^* & - \\ - & \dot{p}_{0,1}^* & - \\ - & \vdots & - \\ - & \dot{p}_{0,N}^* & - \end{bmatrix}, \quad T^{-1} = \begin{bmatrix} | & | & | & | \\ p_{0,0} & p_{0,1} & \cdots & p_{0,N} \\ | & | & | & | \end{bmatrix}. \quad (10)$$

For an orthogonal basis, T^{-1} is equal to T^H where $[\cdot]^H$ is the Hermitian operator. However, the equality of T^H and T^{-1} dictates to use the same Gabor systems at the transmitter and receiver, and it corresponds to choosing $p_{tx}(t) = p_{rx}(t)$.

Extending the concept of orthogonal basis, a collection of basis functions is called as Riesz basis if it is possible to generate a basis via converting the orthogonal basis functions with an invertible linear transformation. Therefore, even though the obtained basis is not constructed with orthogonal

set of functions, i.e., $T^{-1} \neq T^H$, it is possible to obtain another basis where the inner product of the functions selected in those sets yields to $TT^{-1} = I$. In other words, perfect reconstruction is still possible by employing two different Gabor systems where $p_{tx}(t) \neq p_{rx}(t)$ at the transmitter and the receiver. In that case, the Gabor systems, i.e., T and T^{-1} , constitutes a *biorthogonal system*. Since $p_{mk}(t)$ and $\hat{p}_{nl}(t)$ are interchangeable they are called as *dual bases*.

A nice interpretation on orthogonality and biorthogonality is provided in [32]. If an operator, i.e. known as *frame operator*, is defined as $S \triangleq TT^H$, the reconstruction of X_{mk} is given by

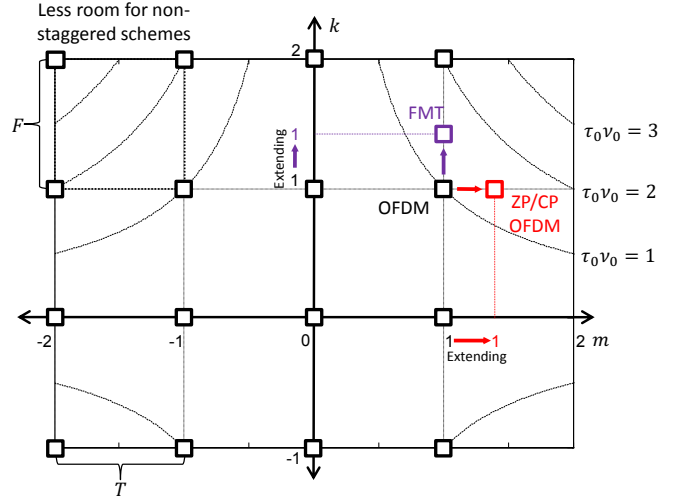
$$\begin{aligned} X_{mk} &= SS^{-1}X_{mk} = S^{-\rho}SS^{-(1-\rho)}X_{mk} \\ &= S^{-\rho}TT^H S^{-(1-\rho)}X_{mk} \\ &= S^{-\rho}T \times \underbrace{(S^{-(1-\rho)}T)^H X_{mk}}_{\text{Transmitted signal}} \\ &= S^{-\rho}T \times \underbrace{(S^{-(1-\rho)}T)^H X_{mk}}_{\text{Received symbol}} \end{aligned} \quad (11)$$

where ρ is the weighting parameter between orthogonality and biorthogonality. While the choice of $\rho \rightarrow 1/2$ yields a more orthogonal system, $\rho \rightarrow 0$ or $\rho \rightarrow 1$ increase the biorthogonality. Note that using orthogonal basis functions, similar to the match filtering, maximizes signal-to-noise ratio (SNR) for AWGN channel. On the contrary, the biorthogonality offers better performance in a dispersive channel. Therefore, it is possible to change the weight on orthogonality-biorthogonality via ρ depending on the dispersiveness of the channel [32].

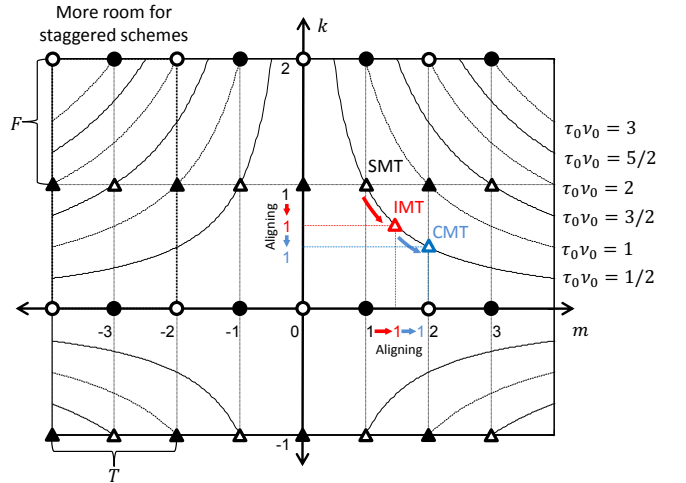
C. Classification of Multicarrier Systems

Considering the theory of Gabor systems, various FBMC schemes are investigated depending on τ_0 , ν_0 , and the information symbols. If complex information symbols are used, it is possible to synthesize three main schemes with perfect reconstruction property; CP/ZP-OFDM and FMT are introduced in Fig. 3(a). OFDM without any guard time is a canonical example when $\tau_0\nu_0 = 1$. However, as indicated before, the well-localized filter cannot be utilized. Thus, employed filters make the system susceptible to the dispersions in the channel. Therefore, ISI is typically handled through the use of a CP. This prevents interference in time domain, at the cost of reduction of spectral efficiency to $\beta/(F(T + T_{CP}))$ by selecting $\nu_0 = F = 1/T$ and $\tau_0 = T + T_{CP}$, where T_{CP} is a cyclic prefix duration to combat with multipath. On the contrary, FMT, which has been proposed before for digital subscriber lines (DSL) applications in [33] and [34], separates the subcarriers by selecting $\nu_0 \geq F$ instead of overlapping adjacent subcarriers. Therefore, FMT can provide same lattice sampling density of CP/ZP-OFDM. However, the guard interval in OFDM and guard bandwidth in FMT do not address the time/frequency spreading in the same manner. While CP-OFDM provides time spreading control along with FDE, FMT does not offer the same degree of freedom for frequency spreading. FMT rather comes into prominence for controlling the out-of-band leakage. Illustrations of OFDM and FMT are given in Fig. 4.

One of the key goals in FBMC systems to control the interferences from other lattice grid points, i.e. ISI and ICI in time



(a) Multicarrier schemes employing in-phase and quadrature components over the same lattice. By extending $\nu_0\tau_0$, the lattices for OFDM with CP or ZP, and FMT-based FBMC can be obtained. The room for the time-frequency localization of the prototype filter depends on $\nu_0\tau_0$. While extending $\nu_0\tau_0$ relaxes the design of the prototype filter, it also degrades the spectral efficiency of the system as in OFDM with CP or ZP and FMT-based FBMC. (\square : Symbols on both quadrature and in-phase components)



(b) Multicarrier schemes employing in-phase and quadrature components over the staggered lattices. All even-symmetric and real prototype filters provides orthogonality among the symbols located on multiple of $\nu_0\tau_0/2$ distances away for in-phase and quadrature components separately. Therefore, the room for the time-frequency localization of the prototype filter is relaxed compared to the schemes that place in-phase and quadrature component over the same lattice. By aligning the places of the symbols, different schemes, i.e. SMT, CMT, and IMT, can be obtained. (\bullet, \blacktriangle : Symbols on quadrature component, \circ, \triangle : Symbols on in-phase component)

Fig. 3: Representations of various multicarrier schemes on time/frequency plane.

and frequency domains, to a certain symbol while maintaining the maximum spectral efficiency. As opposed to extending the lattice, this can be achieved through well-designed prototype filters with using staggered lattices for in-phase and quadrature components. Four different symbol shapes are indicated in Fig. 3(b). As long as the prototype filter is an even and real function, it is guaranteed that there will be no interference among the symbols located on multiples of $\nu_0\tau_0/2$ distances away for in-phase and quadrature components separately (see

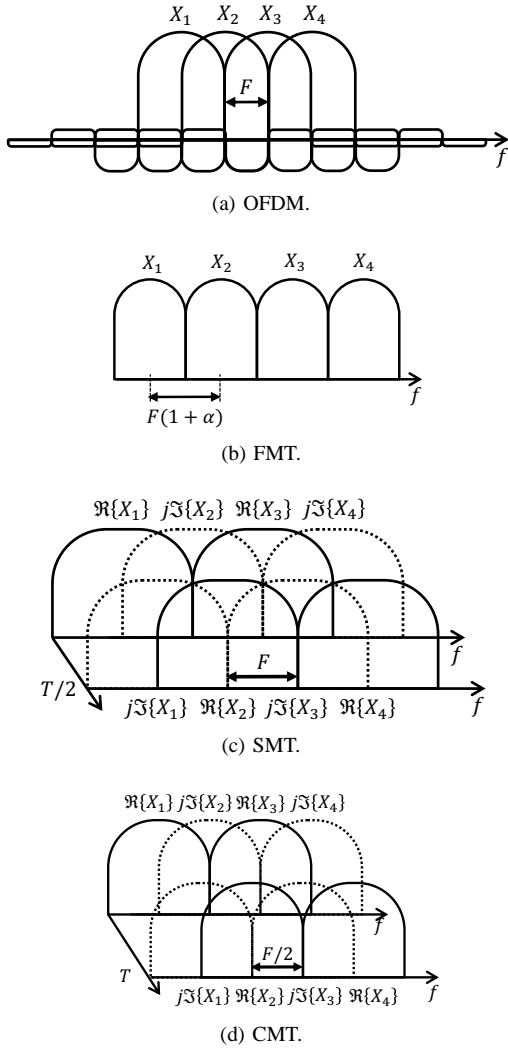


Fig. 4: Illustrations of various multicarrier schemes in time and frequency domains. While OFDM provides the orthogonality by overlapping the sinc-type of functions in frequency domain, FMT provides the orthogonality without overlapping in frequency domain. Both FMT and OFDM can provide the same lattice density with guard band and guard time. On the other hand, SMT and CMT exploits the staggered structures to achieve flexibility on filter design while maintaining the spectral efficiency of $\tau_0\nu_0 = 1$. CMT and SMT can be obtained by exchanging the time and frequency axes.

e.g. [12] for proof). On the other hand, the interference among the other points of the same shape is avoided/minimized through a well-designed prototype filter. A basic comparison on non-staggered and staggered structures can be given as follows:

Observation-I: The lattice density of in-phase component or quadrature component in a staggered structure is equal to the half of the lattice density of non-staggered one. Therefore, staggered structures yield more room for prototype filter design.

Observation-II: The lattice density of a non-staggered structure is equal to the half of the lattice density of staggered one.

However, since complex symbols are transmitted at each grid point in non-staggered structures, both modulation formats have the same spectral efficiency in the absence of a guard interval or band.

According to *Observation-I*, having more room for the filter design in staggered structures allows ISI and ICI to be controlled via well-designed filters. In other words, staggered structures introduce the paradigm of the localizations of the ICI and the ISI with the proper filters while maintaining spectral efficiency. Thus, they indirectly might allow the practical equalizers which exploit the localized ICI and ISI to combat with doubly dispersive channels. However, since there will be *intrinsic* interference between quadrature and in-phase components in a multipath channel, computational complexity becomes the bottleneck for the staggered structures.

Staggering in-phase and quadrature lattices leads two important modes used often in the literature, i.e. SMT and CMT [11]. These two modes are very similar to each other as the points on the lattice have the same product of $\tau_0\nu_0$ as given in Fig. 3(b). The illustrations for SMT and CMT are given in Fig. 4. Indeed, by aligning the position of the pulses in the lattice, it is possible to obtain other modes. For example, a mode which is called IMT in this study can be synthesized by setting as $\tau_0 = \sqrt{2}T/2$ and $\nu_0 = \sqrt{2}F/2$.

In the literature, FBMC approaches are often related with the orthogonal transmission and reception. For example, OFDM without CP, ZP-OFDM which provides a guard period between each OFDM symbols, and FMT, SMT, and CMT based FBMC schemes are based on the orthogonality of the basis functions. However, FBMC can also be extended to biorthogonal schemes which utilize different filters at the transmitter and the receivers [16]. Note that orthogonality is not a requirement for perfect construction, however it provides minimum error caused by AWGN [32]. On the other hand, *biorthogonality* is an important fact that can yield better immunity to doubly dispersive channels compared to the orthogonal systems [16]. Also, it might allow additional relaxations on the equalization complexity. Using an extended rectangular filter at the transmitter and removing the extended part with another rectangular filter as in CP-OFDM is the most prominent example of biorthogonal systems [13], [14]. One can interpret that CP-OFDM benefits from the biorthogonal filter utilization which allows FDE by providing circularity in time domain. While an orthogonal system results in better SIR performance for $\nu_0\tau_0 > 1$ compared to $\nu_0\tau_0 = 1$, a biorthogonal system with optimal pulses can minimize the interference contribution from other information symbols in doubly dispersive channel by allowing different filters at the transmitter and the receiver. Indeed, optimizing the filters subject to the less interference contribution do not consider the equalization complexity. Thus, instead of optimizing the filters for SIR performance solely in doubly dispersive channel, biorthogonal schemes with suboptimum filters can lead simpler equalization, e.g., FDE as in CP-OFDM.

Single-carrier transmissions which allows better PAPR characteristics and FDE along with CP utilization as in single carrier frequency domain equalization (SC-FDE) and single

carrier frequency division multiple accessing (SC-FDMA) schemes [35]–[39] can also be explained with FBMC approaches if one consider an additional filter bank that spreads the energy of the information symbols in frequency domain. In other words, as oppose to use single Gabor system at the transmitter and receiver, two Gabor systems combined with serial-to-parallel conversion at the transmitter and the receiver are employed to yield single carrier systems. For example, SC-FDMA employs filter banks constructed with a rectangular filter to spread (i.e., DFT) and de-spread (i.e., inverse DFT) the information symbols in frequency domain at the transmitter and receiver. On the contrary, in OFDM, since there is no effort on spreading the information symbols in frequency domain, employed prototype filter spreading in frequency domain corresponds to Dirac function. Therefore, considering spreading the information symbols in both time and frequency and biorthogonal/orthogonal schemes, filter bank spread FBMC (FB-S-FBMC), which is only investigated for orthogonal systems in [40], provides a broader transmission and reception framework from mathematical perspective.

III. PROTOTYPE FILTER DESIGN

FBMC allows flexibility on the design of prototype filters considering orthogonal and biorthogonal schemes when $\nu_0\tau_0 > 1$. This flexibility motivates the prototype filter design for different purposes. Goal of this section is to review them, and discuss their trade-offs. The analytical expressions of all filter considered are given in TABLE II. Then, the filters are investigated by classifying them under three main branches considering their theoretical definitions: time-limited filters, band-limited filters, and localized filters.

A. Time-limited Filters

Time-limited filters consist of the filters where their theoretical definitions are given for finite durations as the name implies. The spectrum of these filters have infinite length due to the finite durations. Since they are specifically design for finite duration, they provide easy implementations of the systems.

1) *Rectangular Filter*: Rectangular prototype filter is defined by [12]. It is the prototype filter used in OFDM. If the rectangular filter is extended by T_{CP} , conventional CP utilization is obtained. Also, it is possible to control the spectral leakage of the rectangular filter by introducing additional windowing periods [41]. Extending the rectangular filter allows multipath delay spread immunity. However, this approach is likely to be a suboptimal solution under doubly dispersive channels, since this approach does not treat the time and frequency dispersions equally [16].

2) *Hamming, Hanning and Blackman Filters*: In [11], Hamming, Hanning, and Blackman windows (see also [42], [43]) are specified with K_1 , K_2 , K_3 respectively denoting the normalizing coefficients to satisfy the following constraint

$$\begin{cases} \int_0^{T_0} p(t)dt = 1, & 0 \leq t \leq T_0, \\ p(t) = 0, & t < 0 \text{ and } t > T_0. \end{cases} \quad (12)$$

where T_0 is the duration of the filter.

3) *Optimal Finite Duration Pulses/Prolate*: In FBMC systems, filters have to be truncated because of the computational complexity which is directly proportional to the filter length. However, using shorter or truncated filter causes undesired sidelobes in frequency domain as in rectangular and truncated RRC filters. As a tempting solution for this trade-off, achieving a time-limited pulse with minimum sidelobe power constitutes the main motivation of prolate spheroidal wave functions (PSWFs). The set of prolate functions can span the Hilbert space $\mathcal{L}^2(\mathbb{R})$ of square-integrable functions. In other words, PSWF constructs a complete set of functions. In order to achieve better understanding of the PSWFs, first, *discrete prolate sequences*, which are also called as Slepian sequences have to be investigated. Two main features of these sequences are distinctive compared to other basis;

- These sequences are orthonormal for a given sequence length. This is also true for fundamental basis, i.e., sine and cosine as in Fourier transformation between $0 - 2\pi$. However, the sequence length is an input parameter for Slepian sequences. This is important since the length of the sequences corresponds to the truncation or a finite duration pulses in communication systems.
- These sequence are eigenfunctions of a perfect low pass filter. Therefore, these sequences can pass through a low pass filter without any distortion or filtering effect excluding the scaling with a real coefficient, i.e., eigenvalues, which corresponds to the energy in that bandwidth. Assuming that the energy of the pulse is 1, eigenvalues will always be less than 1.

These two features mean that if one provides the filter length and the bandwidth where the pulse has to fit as the design constraints, the optimum pulse becomes the function which has the maximum eigenvalue in the set constructed with these constraints. It is worth to note that since the functions are orthogonal to each other, the strongest eigenfunction is favorable compared to the others. This issue is explained as a sidelobe minimization problem in [11] as

$$\hat{p}(t) = \underset{p(t)}{\operatorname{argmin}} \left\{ \int_{-\infty}^{\infty} |P(f)|^2 df - \int_{-\Delta f/2}^{\Delta f/2} |P(f)|^2 df \right\}. \quad (13)$$

However, even if the sequence with maximum eigenvalue is optimum in terms of sidelobe for a given filter length, it does not solely satisfy the Nyquist criterion ensuring zero ICI and ISI. Considering this fact, Vahlin exploits PSWFs to realize a new family which is called as optimal finite duration pulse (OFDP) [44] by generalizing the optimization procedure for single carrier presented in [45]. Basically, the aim is to achieve a Nyquist filter in both time and frequency with the maximum energy in the main lobe for a given bandwidth and filter length. In order to develop these pulses, Vahlin chooses the signal representation as the linear combinations of the PSWFs. Indeed, another basis can be selected to construct these pulses. However, the required number of basis function might be very high. Vahlin formulates the constraints as an optimization problem to find the weights (a_k) for k th PSWF ($\psi_{k,\text{prolate}}(t)$) truncated to interval $[-(K/2)T, (K/2)T]$ using Lagrange mul-

TABLE II: Analytical expressions of well-known prototype filters in the literature.

Family	Filter	Analytical Model	Parameters
Time-limited	Rectangular	$p_{\text{rec}}(t) = \begin{cases} \frac{1}{\sqrt{T}}, & t \leq \frac{T}{2} \\ 0, & \text{otherwise} \end{cases}$	-
	Ext. rectangular	$p_{\text{erec}}(t) = \begin{cases} \frac{1}{2\sqrt{T}} + \frac{1}{2\sqrt{T}} \cos(\pi \frac{ t - \frac{T}{2} - T_{\text{CP}}}{T_W}), & -\frac{T}{2} - T_{\text{CP}} - T_W \leq t < -\frac{T}{2} - T_{\text{CP}} \\ \frac{1}{\sqrt{T}}, & -\frac{T}{2} - T_{\text{CP}} \leq t \leq \frac{T}{2} \\ \frac{1}{2\sqrt{T}} + \frac{1}{2\sqrt{T}} \cos(\pi \frac{ t - \frac{T}{2}}{T_W}), & \frac{T}{2} < t \leq \frac{T}{2} + T_W \\ 0, & \text{otherwise} \end{cases}$	$0 \leq T_{\text{CP}},$ $0 \leq T_W$
	Hamming	$p_{\text{hamm}}(t) = K_1 \left(0.54 - 0.46 \cos\left(\frac{2\pi t}{T_0}\right) \right) \Pi\left(\frac{t - T_0/2}{T_0}\right)$	-
	Hanning	$p_{\text{hann}}(t) = K_2 \left(0.5 - 0.5 \cos\left(\frac{2\pi t}{T_0}\right) \right) \Pi\left(\frac{t - T_0/2}{T_0}\right)$	-
	Blackman	$p_{\text{blackman}}(t) = K_3 \left(0.42 - 0.5 \cos\left(\frac{2\pi t}{T_0}\right) + 0.08 \cos\left(\frac{4\pi t}{T_0}\right) \right) \Pi\left(\frac{t - T_0/2}{T_0}\right)$	-
	OFDP/Prolate	$p_{\text{ofdp}}(t) = \sum_{k=0}^{N_p} a_{2k} \psi_{2k, \text{prolate}}(t)$	N_p, K
	Kaiser	$p_{\text{kaiser}}(t) = \begin{cases} I_0(\beta \sqrt{1 - (2n/N)^2}) / I_0(\beta), & -\frac{N}{2} \leq n \leq \frac{N}{2} \\ 0, & \text{otherwise} \end{cases}$	β
Band-limited	PHYDYAS	$p_{\text{phydyas}}(t) = \begin{cases} 1 + 2 \sum_{k=1}^{K-1} a_k \cos\left(2\pi \frac{kt}{Kt}\right), & -\frac{KT}{2} \leq t \leq \frac{KT}{2}, \\ 0, & \text{otherwise} \end{cases}$ $P_{\text{phydyas}}(f) = \sum_{k=-(K-1)}^{K-1} a_k \frac{\sin\left(\pi\left(f - \frac{k}{MK}\right)\right)}{MK \sin\left(\pi\left(f - \frac{k}{MK}\right)\right)}$	K
	RC	$p_{\text{rc}}(t) = \frac{\sin(\pi t/T_s) \cos(\pi \alpha t/T_s)}{\pi t/T_s \sqrt{1 - 4\alpha^2 t^2/T_s^2}}$ $P_{\text{rc}}(f) = \begin{cases} T_s, & f \leq \frac{1-\alpha}{2T_s} \\ \frac{T_s}{2} \left(1 + \cos\left(\frac{\pi T_s}{\alpha} \left(f - \frac{1-\alpha}{2T_s}\right)\right) \right), & \frac{1-\alpha}{2T_s} \leq f \leq \frac{1+\alpha}{2T_s} \\ 0, & \text{otherwise} \end{cases}$	$0 \leq \alpha_r \leq 1$
	RRC	$p_{\text{rrc}}(t) = \begin{cases} 1 - \alpha_r + 4\frac{\alpha_r}{\pi}, & t = 0 \\ \frac{\alpha_r}{\sqrt{2}} \left[\left(1 + \frac{2}{\pi}\right) \sin\left(\frac{\pi}{4\alpha_r}\right) + \left(1 - \frac{2}{\pi}\right) \cos\left(\frac{\pi}{4\alpha_r}\right) \right], & t = \pm \frac{T}{4\alpha_r} \\ \frac{\sin\left((1-\alpha_r)\frac{\pi t}{T}\right) + 4\frac{\alpha_r t}{T} \cos\left((1+\alpha_r)\frac{\pi t}{T}\right)}{\frac{\pi t}{T} \left(1 - \frac{16\alpha_r^2 t^2}{T^2}\right)}, & \text{otherwise} \end{cases}$ $P_{\text{rrc}}(f) = \sqrt{P_{\text{rc}}(f)}$	$0 \leq \alpha_r \leq 1$
	Half sinc	RRC ($\alpha_r = 0$)	
Localized	Half cosine	RRC ($\alpha_r = 1$)	
	Gaussian	$p_{\text{gaussian}}(t) = (2\alpha_g)^{1/4} e^{-\pi \alpha_g t^2}, \quad P_{\alpha_g}(f) = p_{\text{gaussian}}(t, 1/\alpha_g)$	$0 < \alpha_g$
	Hermite	$p_{\text{hermite}}(t) = \sum_{k=0}^{N_H} a_{4k} \psi_{4k, \text{hermite}}(t),$ $\psi_{n, \text{hermite}}(t) = H_n(\sqrt{2\pi}t) e^{-\pi t^2}, \quad H_n(t) = (-1)^n e^{t^2} \frac{d^n}{dt^n} e^{-t^2}$	N_H
	IOTA	$p_{\text{iota}}(t) = \mathcal{F}^{-1} \mathcal{O}_{\tau_0} \mathcal{F} \mathcal{O}_{v_0} p_{\text{gsn}}(t, \alpha)$ $\mathcal{O}_a x(t) = \frac{x(t)}{\sqrt{a \sum_{k=-\infty}^{\infty} \ x(t - ka)\ ^2}}, \quad x(t) \in \mathbb{R}$ $\mathcal{F}^{-1} X(f) = \int X(f) e^{-j2\pi f t} df, \quad \mathcal{F} x(t) = \int x(t) e^{j2\pi f t} dt$	$0 < \alpha_g$
	EGF	$p_{\text{egf}}(t) = \frac{1}{2} \left[\sum_{k=0}^{\infty} d_{k, \alpha, v_0} \left[p_{\text{gaussian}}(t + k/v_0, \alpha) + p_{\text{gaussian}}(t - k/v_0, \alpha) \right] \right] \times$ $\sum_{l=0}^{\infty} d_{l, 1/\alpha, \tau_0} \cos(2\pi l t / \tau_0)$	-

multipliers and calculus of variations. Note that since only even indexed prolate functions are even-symmetrical, only a_{2k} are considered through the optimization procedure. By applying similar optimization procedure, OFDP has been utilized in other studies [9]. Also, another optimization procedure which is based on deriving the composite Nyquist response of OFDP filter instead OFDP itself is suggested in [46] to reduce the optimization complexity in [44].

4) *Kaiser Filter*: Another efficient solution for a filter with finite length is proposed by Jim Kaiser by employing Bessel Functions to achieve an approximation to the PSWFs [47], [48]. Basically, it offers a suboptimal solution for the out-of-band leakage. A favorable property of Kaiser filter is its flexibility to control the sidelobes and stop-band attenuation, through a single design parameter β . The expression is given in TABLE II where N is the filter order, $I_0(x) = 1 + \sum_{k=1}^{\infty} \left[\frac{(x/2)^k}{k!} \right]^2$ denotes the modified zeroth order Bessel

TABLE III: PHYDYAS filter coefficients for different overlapping factors [50].

	$K = 3$	$K = 4$	$K = 6$	$K = 8$
a_0	1	1	1	1
a_1	-0.91143783	-0.97195983	-0.99722723	-0.99988389
a_2	+0.41143783	+0.70710681	+0.94136732	+0.99315513
a_3		-0.23514695	-0.70710681	-0.92708081
a_4			+0.3373834	+0.70710681
a_5			-0.07441672	-0.37486154
a_6				+0.11680273
a_7				-0.01523841

function. To achieve a minimum stop-band attenuation of α_{sb} dB, value of β may be selected as follows [49]

$$\beta = \begin{cases} 0.1102(\alpha_{\text{sb}} - 8.7), & \alpha_{\text{sb}} > 50, \\ 0.5842(\alpha_{\text{sb}} - 21)^{0.4} + 0.07886(\alpha_{\text{sb}} - 21), & 21 \leq \alpha_{\text{sb}} \leq 50, \\ 0, & \alpha_{\text{sb}} < 21. \end{cases} \quad (14)$$

Moreover, choosing $N \approx \frac{\alpha - 7.95}{14.36 \Delta f_{\text{trns}}}$ yields a transition band of Δf_{trns} .

5) *PHYDYAS Filter*: A time-domain filter with good frequency localization has been specified in [50] where the coefficients a_k for different filter lengths are specified in TABLE III. The frequency response of this filter is given by [51]. PHYDYAS filter has been investigated further in [10], and was then subsequently adopted to be used in the European PHYDYAS project on FBMC [10], [51], [52].

B. Band-limited Filters

These filters are theoretically defined with finite bandwidth support. However, they theoretically require infinite filter length in time domain. Therefore, these filter are problematic considering practical slot and frame formation.

1) *Raised Cosine Filter*: Raised-cosine filter is a commonly used Nyquist filter in which the time-frequency localization is controlled by a parameter that is referred as the roll-off factor (α_r). While raised cosine filter results in rectangular shape in frequency domain for $\alpha_r = 0$, the filter shape becomes half part of the cosine function when $\alpha_r = 1$. The filter bandwidth is calculated by $(1 + \alpha_r)/T$ without any filter truncation.

2) *Root-Raised Cosine Filter*: Typically, RRC filter used at the transmitter and receiver to satisfy Nyquist criterion is derived from raised-cosine filter. If the frequency response of RRC filter is given by $P_{\text{rrc}}(f)$, then, the relation $P_{\text{rc}}(f) = P_{\text{rrc}}(f)P_{\text{rrc}}(f)$ is obtained.

3) *Half Cosine and Half Sinc Filters*: RRC filter with $\alpha_r = 1$ yields half cosine filter (HCF), which is given by [8], [9], [11], [53], [54]. The half cosine filter provides a good compromise for time/frequency behavior; its relaxed transition bands allow approximation through a relatively short time-domain filter, while achieving high attenuation in the stop-band [11]. On the other hand, RRC filter with $\alpha_r = 0$ is called as half sinc pulse. While half sinc results in minimal bandwidth, it is very susceptible to the filter truncation.

C. Localized Filters

In contrast to the finite support in one domain as in time-limited and band-limited filters, localized filters consider both domains on an equal footing. Therefore, they try to provide the compactness in both time and frequency domains. They can give the isotropic (same) responses in time and frequency domains. They tend to behave as a Gaussian pulse because of its maximum compactness.

1) *Gaussian Filter*: Gaussian filter is given by [12], [54]–[57] with a control parameter α_g . Using the properties of Fourier transform, one may show that the frequency response of a Gaussian function is also another Gaussian function [12]. If $\alpha_g = 1$, Gaussian filter is perfectly isotropic. On the other hand, since $p_{\text{gaussian}}(t) > 0$ for all t , Gaussian filter does not satisfy Nyquist criterion. In other words, it causes ICI/ISI from a certain symbol to its neighboring lattice grid points in Fig. 3.

2) *Hermite Pulses*: Hermite functions have been commonly used in the literature to obtain well-localized pulse shapes in doubly dispersive channels [16], [17], [20], [57], [58]. They are obtained from Hermite polynomial functions $H_n(t)$ of different orders n which can span the space Hilbert space $\mathcal{L}^2(\mathbb{R})$ of square-integrable functions. Note that Hermite pulses of different orders are orthogonal to each other with respect to the weight function $e^{-\pi t^2}$. Therefore, by deforming the Gaussian filter with higher order Hermite functions, zero crossings in time are provided to satisfy Nyquist criterion. The general filter design approach based on Hermite functions is to linearly combine weighted versions of Hermite pulses with different orders which provide isotropic dispersion in time and frequency domains [59] in order to obtain a prototype filter that will perform best for a given channel environment [17], [20], [57]. Also, employing the orthogonality between Hermite functions, concentric toroidal pulses are introduced to increase the spectral efficiency of the transmission [58].

3) *Isotropic Orthogonal Transform Algorithm Filter*: The isotropic orthogonal transform algorithm (IOTA) filter targets to preserve the excellent localization property of Gaussian prototype filter, and orthogonalizes it to prevent ISI and ICI to neighboring symbols in time/frequency lattice. Starting with the Gaussian function, orthogonalized pulse is obtained as shown in TABLE II where \mathcal{F} and \mathcal{F}^{-1} are the operators for Fourier transform and its inverse, respectively, $\|\cdot\|$ is L^2 -norm, and \mathcal{O}_a is an orthogonalization operator on a function. The resulting prototype filter fulfills the Nyquist criterion. For $\alpha = 1$, $\tau_0 = \sqrt{2}T/2$ and $\nu_0 = \sqrt{2}F/2$, $p_{\text{iota}}(t)$ becomes identical to its Fourier transform, and therefore becomes an isotropic filter. With these parameters, IOTA filter corresponds to optimal Nyquist filter in terms of time-frequency localization when the rectangular lattice is considered. [32].

4) *Extended Gaussian Function*: Extended Gaussian function has a closed-form expression given by [60] with $\tau_0 \nu_0 = 0.5$, $0.528\nu_0^2 \leq \alpha \leq 7.568\nu_0^2$, and real valued coefficients d_{k,α,ν_0} can be computed (for finite number of coefficients $b_{k,j}$)

as [61]

$$d_{k,\alpha,\nu_0} = \sum_{j=0}^{j_k} b_{k,j} e^{-(\pi\alpha/2\nu_0^2)(2j+k)} , \quad 0 \leq k \leq K , \quad (15)$$

where [61] lists the coefficients $b_{k,j}$ for $0 \leq k \leq 14$ and $0 \leq j \leq 7$. Note that similar to the relation in Gaussian function, EGF has the same shape with its Fourier transform, except a scaling term [62]. Two special cases of EGF are as follows [60]:

- IOTA: For $\alpha = 1$, $\tau_0 = \sqrt{2}T/2$ and $\nu_0 = \sqrt{2}F/2$, EGF becomes the IOTA filter.
- TFL1: When EGF is truncated (e.g., into one symbol duration – and hence the naming TFL1), modulation/demodulation delay may be shortened, and good time-frequency localization can be still maintained through some optimization procedures [63]–[66].

IV. TOOLS FOR PROTOTYPE FILTER ANALYSES

In order to better understand the impact of prototype filters in FBMC schemes, various tools and metrics are introduced in this section. Use of these tools will be instrumental for assessing the performances of different prototype filters.

A. Time-Frequency Localization

It basically states that a narrow waveform yields a wide spectrum or a wide waveform results in a narrow spectrum, and making narrow in both domains is not possible. Time-frequency localization of a filter is measured by Heisenberg uncertainty parameter ξ_{filter} which is given by

$$\xi_{\text{filter}} \equiv \frac{\|p(t)\|^2}{4\pi\sigma_t\sigma_f} \leq 1 , \quad (16)$$

where

$$\sigma_t = \sqrt{\int_{\mathbb{R}} (t - \bar{t})^2 |p(t)|^2 dt} , \quad (17)$$

$$\sigma_f = \sqrt{\int_{\mathbb{R}} (f - \bar{f})^2 |P(f)|^2 df} , \quad (18)$$

σ_t is the time dispersion (or the standard deviation of the pulse in time), and σ_f is the frequency dispersion (or the standard deviation of the pulse in frequency), and \bar{t} and \bar{f} are arbitrary real numbers² [11], [12], [32].

B. Direction Parameter

The direction parameter $\kappa \in [0, \infty)$, which shows how a pulse shape lies in time-frequency plane, is given in [54] as

$$\kappa = \frac{\sigma_t}{\sigma_f} . \quad (19)$$

For example, while κ is equal to 0 for the rectangular filter, Gaussian filter with $\alpha_g = 1$ gives $\kappa = 1$ because of its isotropic dispersion. Larger κ means a pulse stretched more along the time axis compared to the frequency axis.

² \bar{t} and \bar{f} are not necessarily the mean values of the pulse in time and frequency, respectively.

C. Ambiguity Function

Generalized Nyquist criterion, discussed in more detail in [8], [12], [49], [53], [60], [61], states that the projection of transmitter and receiver prototype filters should be zero at every integer multiple of symbol spacing in both time and frequency as

$$\langle p_{mk}(t), \dot{p}_{nl}(t) \rangle = \int_{-\infty}^{\infty} p_{tx}(t - m\tau_0) p_{rx}^*(t - n\tau_0) e^{-j2\pi(l-k)\nu_0 t} dt = \delta_{mn} \delta_{lk} . \quad (20)$$

By using fractional values instead of using integer multiples, equation given in (20) also leads to a more generalized form, known as the ambiguity function [17], [54]

$$A_{\mathcal{R}}(\phi, \psi) \triangleq \int_{-\infty}^{\infty} p_{tx}^*\left(t - \frac{\phi}{2}\right) p_{rx}\left(t + \frac{\phi}{2}\right) e^{-j2\pi\psi t} dt . \quad (21)$$

The properties of ambiguity function are given below:

- Ambiguity function is a two dimensional correlation function in the time-frequency plane.
- Ambiguity function yields real values in the case of an even-symmetric prototype filters.
- Generalized Nyquist criterion can also be expressed in terms of the ambiguity function as

$$A_{\mathcal{R}}(n\tau_0, l\nu_0) = \begin{cases} 1 , & n = l = 0 \\ 0 , & \text{otherwise} \end{cases} . \quad (22)$$

- Ambiguity function characterizes the amount of interference that leaks into other symbols in the time-frequency grid. Ambiguity function gives an intuitive demonstration of ICI/ISI robustness. It indicates the sensitivity to time and frequency impairments.
- Similar to time-frequency localization of a filter, ambiguity function also cannot be concentrated arbitrarily. The limitation is given by [32]

$$\xi_{\text{ambiguity}} \equiv \frac{\|p_{tx}(t)\|^2 \|p_{rx}(t)\|^2}{2\pi\sigma_\phi\sigma_\psi} \leq 1 , \quad (23)$$

where

$$\sigma_\phi = \sqrt{\iint_{\mathbb{R}} (\phi - \bar{\phi})^2 |A_{\mathcal{R}}(\phi, \psi)|^2 d\phi d\psi} , \quad (24)$$

$$\sigma_\psi = \sqrt{\iint_{\mathbb{R}} (\psi - \bar{\psi})^2 |A_{\mathcal{R}}(\phi, \psi)|^2 d\phi d\psi} , \quad (25)$$

and, $\bar{\phi}$ and $\bar{\psi}$ are arbitrary real numbers.

In the literature, ambiguity function is also used to obtain other functions. For example, interference function which is defined by

$$I(\phi, \psi) = 1 - |A_{\mathcal{R}}(\phi, \psi)|^2 \quad (26)$$

might provide better visualization on ICI and ISI [12], [60]. In order to simplify the expressions of average SIR due to

dispersion in the channel, $A_{\mathcal{R}}(\phi, \psi)$ is changed by introducing additional phase shift ρ as

$$A(\phi, \psi) \triangleq e^{-j2\pi\rho} \int_{-\infty}^{\infty} p_{\text{tx}}(t - \phi) p_{\text{rx}}^*(t) e^{j2\pi\psi t} dt, \quad (27)$$

where $A(\phi, \psi)$ is the modified ambiguity function. $A_{\mathcal{R}}(\phi, \psi)$ can be derived as $A_{\mathcal{R}}(\phi, \psi) = A^*(\phi, \psi) \big|_{\rho=\psi\phi/2}$.

D. Orthogonality Parameter

The reconstruction quality of the prototype filter which is investigated by the orthogonality parameter of σ_I^2 [54] given by

$$\sigma_I^2 = \mathbb{E} \left\{ \left| X_{nl} - \tilde{X}_{nl} \right|^2 \right\}. \quad (28)$$

Using (28), it is possible to write the average SIR performance as

$$SIR = \frac{\sigma_S^2}{\sigma_I^2}, \quad (29)$$

where σ_S^2 and σ_I^2 are the power of the desired part and the interference leaking from other symbols, respectively. SIR, as defined here, should ideally be infinity, since no other interference sources are considered. However, orthogonality can be still spoiled by not only due to the lack of exact representation of the filter in digital domain, but also due to the doubly dispersive channels. In the literature, statistical characteristics of the channel are generally described with wide-sense stationary uncorrelated scattering (WSSUS) assumption [130] given by

$$\mathbb{E} \{ H(\tau, \nu) \} = 0, \quad (32)$$

$$\mathbb{E} \{ H(\tau, \nu) H^*(\tau_1, \nu_1) \} = S_H(\tau, \nu) \delta(\tau - \tau_1) \delta(\nu - \nu_1), \quad (33)$$

where $S_H(\tau, \nu)$ is the channel scattering function. The term of *wide sense stationary* ensures the autocorrelation is stationary. In other words, static characteristics of the channel do not change in time, and are only related with time difference as in (33). The term of *uncorrelated scattering* shows that one of the delay components of the received signal is uncorrelated with all the other delay components. However, note that the WSSUS assumption ignores the non-stationary characteristics due to the distance dependent path loss, shadowing, delay drift, and the correlation between the reflected rays from the same physical objects [131]. In addition, WSSUS assumption is not valid for short-term channel characteristics, especially, when the specular reflections dominate over diffuse scattering [132]. Yet, WSSUS assumption is widely used in the system models to characterize the wireless channels because of its simplicity. For example, exponential decaying multipath with Jakes Doppler spectrum [133] or ITU models [134] for different environments are commonly used for the channel scattering function for terrestrial communications. Considering WSSUS assumption, analytical expressions of σ_S^2 and σ_I^2 also can be obtained for OFDM/QAM and OFDM/OQAM as follows:

1) *SIR for OFDM/QAM*: For OFDM/QAM, $p_{mk}(t)$ and $\dot{p}_{nl}(t)$ can be expressed as

$$p_{mk}(t) = p_{\text{tx}}(t - m\tau_0) e^{j2\pi k\nu_0 t}, \quad (34)$$

$$\dot{p}_{nl}(t) = p_{\text{rx}}(t - n\tau_0) e^{j2\pi l\nu_0 t}, \quad (35)$$

respectively, where $\tau_0\nu_0 = 1$ as in Fig. 3(a). Then, assuming the impact of ICI and ISI on each subcarrier is statistically equal to each other and all subcarriers are utilized, H_{nlmk} can be written as

$$H_{mk} = H_{nlmk} \Big|_{\substack{l=0 \\ n=0}} = \int_{\tau} \int_{\nu} H(\tau, \nu) \times e^{-j2\pi k\nu_0 \tau} \int_t p_{\text{tx}}(t - m\tau_0 - \tau) p_{\text{rx}}^*(t) e^{j2\pi(k\nu_0 + \nu)t} dt d\nu d\tau. \quad (36)$$

Therefore, selecting $\rho = k\nu_0\tau$, (36) is simplified to

$$H_{mk} = \int_{\tau} \int_{\nu} H(\tau, \nu) A(m\tau_0 + \tau, k\nu_0 + \nu) d\nu d\tau. \quad (37)$$

If X_{mk} are independent identically distributed with zero mean and $\langle p_{\text{tx}}(t), p_{\text{rx}}(t) \rangle = 1$, the power of desired part and the power of interference from other symbols are obtained as

$$\sigma_S^2 = \mathbb{E} \left\{ |X_{00}H_{00}|^2 \right\} = \int_{\tau} \int_{\nu} S_H(\tau, \nu) |A(\tau, \nu)|^2 d\nu d\tau, \quad (38)$$

$$\begin{aligned} \sigma_I^2 &= \mathbb{E} \left\{ \left| \tilde{X}_{00} - X_{00}H_{00} \right|^2 \right\} \\ &= \sum_{(m,k) \neq (0,0)} \int_{\tau} \int_{\nu} S_H(\tau, \nu) |A(m\tau_0 + \tau, k\nu_0 + \nu)|^2 d\nu d\tau, \end{aligned} \quad (39)$$

respectively, where $\mathbb{E} \{ \cdot \}$ is the expected value operator.

The illustration of (39) is given in Fig. 5(a), where the absolute value of the ambiguity function at the grid points (black circles) are equal to zero in single-tap channel with no Doppler spread. Due to multipath and Doppler spread (captured by the illustrated scattering function), the desired symbol (red circle) observes ISI/ICI from neighboring grid points.

2) *SIR for FBMC/OQAM*: For FBMC/OQAM, which is a variation of FBMC, $p_{mk}(t)$ and $\dot{p}_{nl}(t)$ can be expressed as

$$p_{mk}(t) = j^{m+k} p_{\text{tx}}(t - m\tau_0) e^{j2\pi k\nu_0 t}, \quad (40)$$

$$\dot{p}_{nl}(t) = j^{n+l} p_{\text{rx}}(t - n\tau_0) e^{j2\pi l\nu_0 t}, \quad (41)$$

respectively, where $\tau_0\nu_0 = 1/2$. Using (40) and (41), (7) can be expressed as

$$\begin{aligned} H_{mk} &= H_{nlmk} \Big|_{\substack{l=0 \\ n=0}} \\ &= j^{m+k} \int_{\tau} \int_{\nu} H(\tau, \nu) A(m\tau_0 + \tau, k\nu_0 + \nu) d\nu d\tau. \end{aligned} \quad (42)$$

Therefore, σ_S^2 and σ_I^2 are obtained as in (43) and (44), respectively, where $\Im \{ \cdot \}$ expresses the imaginary part of argument. By calculating $\Re \{ A(\phi, \psi) \}$ and $\Im \{ A(\phi, \psi) \}$, the impact of

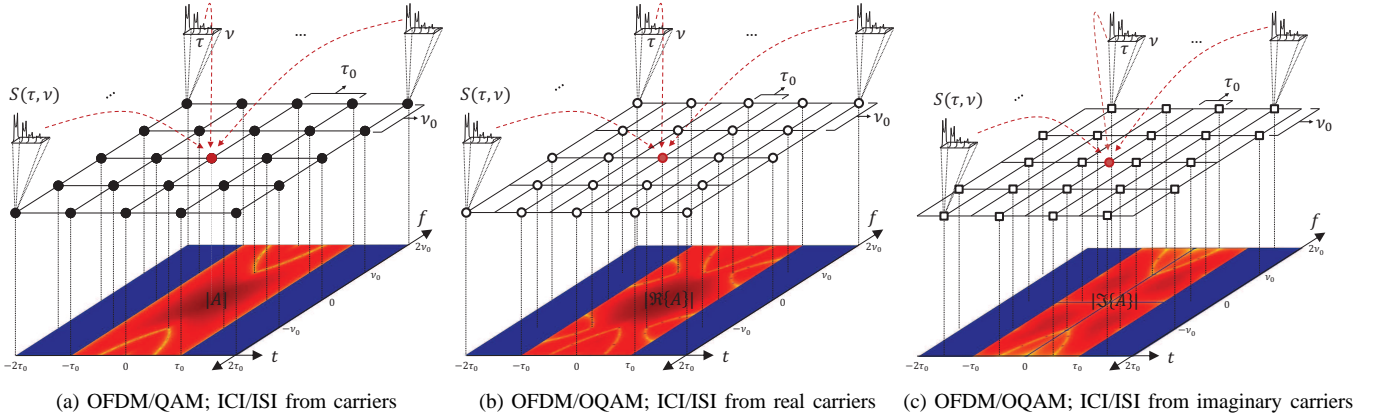


Fig. 5: SIR Calculations for OFDM/QAM and OFDM/OQAM.

$$\sigma_S^2 = \mathbb{E} \{ |\Re \{ X_{00} H_{00} \}|^2 \} = \int_{\tau} \int_{\nu} S_H(\tau, \nu) |\Re \{ A(\tau, \nu) \}|^2 d\nu d\tau, \quad (43)$$

$$\begin{aligned} \sigma_I^2 &= \mathbb{E} \left\{ \left| \tilde{X}_{00} - X_{00} H_{00} \right|^2 \right\} = \sum_{\{m,k\} \neq \{0,0\}} \int_{\tau} \int_{\nu} S_H(\tau, \nu) \left| \Re \{ j^{m+k} A(m\tau_0 + \tau, k\nu_0 + \nu) \} \right|^2 d\nu d\tau \\ &= \left[\sum_{\substack{(m,k) \neq (0,0) \\ m+k \in \text{Even}}} \int_{\tau} \int_{\nu} S_H(\tau, \nu) |\Re \{ A(m\tau_0 + \tau, k\nu_0 + \nu) \}|^2 d\nu d\tau + \sum_{\substack{(m,k) \neq (0,0) \\ m+k \in \text{Odd}}} \int_{\tau} \int_{\nu} S_H(\tau, \nu) |\Im \{ A(m\tau_0 + \tau, k\nu_0 + \nu) \}|^2 d\nu d\tau \right] \quad (44) \end{aligned}$$

the interference from real (i.e. $\text{mod}\{m+k, 2\} = 0$) and imaginary (i.e. $\text{mod}\{m+k, 2\} = 1$) carriers in a doubly dispersive channel environment can be visualized on time-frequency grid as in Fig. 5(b) and Fig. 5(c).

V. EVALUATING PROTOTYPE FILTERS

In this section, comparisons of the prototype filters described in Section III are presented. First, time-frequency characteristics of the filters and the power contribution to the other symbols in frequency domain are given in Fig. 6. Then, the spectral leakage performances of the filters in multicarrier scheme are given in Fig. 7(a) and Fig. 7(b) for 5 MHz and 20 MHz bandwidth utilizations in LTE. While 300 and 1200 subcarriers are utilized for $\nu_0 = F$, proportionally, 424 and 1698 subcarriers are used for $\nu_0 = F/\sqrt{2}$. The ambiguity surfaces of the filters are provided in Fig. 8 to visualize both ICI and ISI. Considering both OQAM and QAM, SIR in (29) plots are given in Fig. 9 for different prototype filters. In addition, the impact of truncation on SIR is investigated for band-limited and localized pulses, which can be seen in Fig. 10. In all other figures, K is fixed to 16 for the sake of implementation purposes unless otherwise stated. Also, the energies of the filters are normalized to 1.

Time-frequency lattice is adjusted considering the staggering strategy of in-phase and quadrature components. For example, symbols are placed to the lattice where $\tau_0 = T$ and $\nu_0 = F$ for rectangular filter in non-staggered structures. Additionally, rectangular filter with CP and windowing ($T_{CP} = T_W = 0.14T$) is included to compare the conventional OFDM with FBMC with the other filters. On the other hand,

while τ_0 and ν_0 are set to $\sqrt{2}T/2$ and $\sqrt{2}F/2$, for Gaussian, Hermite, and IOTA filters ($\alpha_g = 1$), $\tau_0 = \sqrt{2}T/2$ and $\nu_0 = \sqrt{2}F/2$, respectively, the lattice where $\tau_0 = T/2$ and $\nu_0 = F$ is constructed for RRC ($\alpha_r = 0.22$), half sinc (RRC where $\alpha_r = 0$), half cosine (RRC where $\alpha_r = 1$), prolate, and OFDP.

In Fig. 9, SIR plots are obtained by taking four channel scattering models into account; 1) Carrier frequency offset, 2) Timing offset, 3) ITU Vehicular A model with Jake's Doppler spreading, and 4) ITU Pedestrian A model with Jake's Doppler spreading. For ITU channel models, modified Jake's Doppler spectrum, which also includes the time variation of the phase components of the reflected radio waves [135], is applied in order to prohibit the infinite density at the spectrum. In this model, correlation between phase components is defined with B parameter which is a positive constant. In the simulations, heuristically, B is set to $0.5f_d$ where f_d is the maximum Doppler shift.

A. Time-limited Filters

Rectangular prototype filter corresponds to sinc function in frequency domain as given in Fig. 6. Therefore, OFDM has high sidelobes as given in Fig. 7(a) and Fig. 7(b). It is possible to suppress the sidelobes of OFDM by applying proper windowing. However, the spectral leakage of the rectangular pulse is still considerable compared to the other filters. Note that the sidelobes are naturally suppressed in FBMC approaches without sacrificing the spectral efficiency.

In terms of SIR, extended rectangular filter, which corresponds to conventional OFDM, provides the best performance

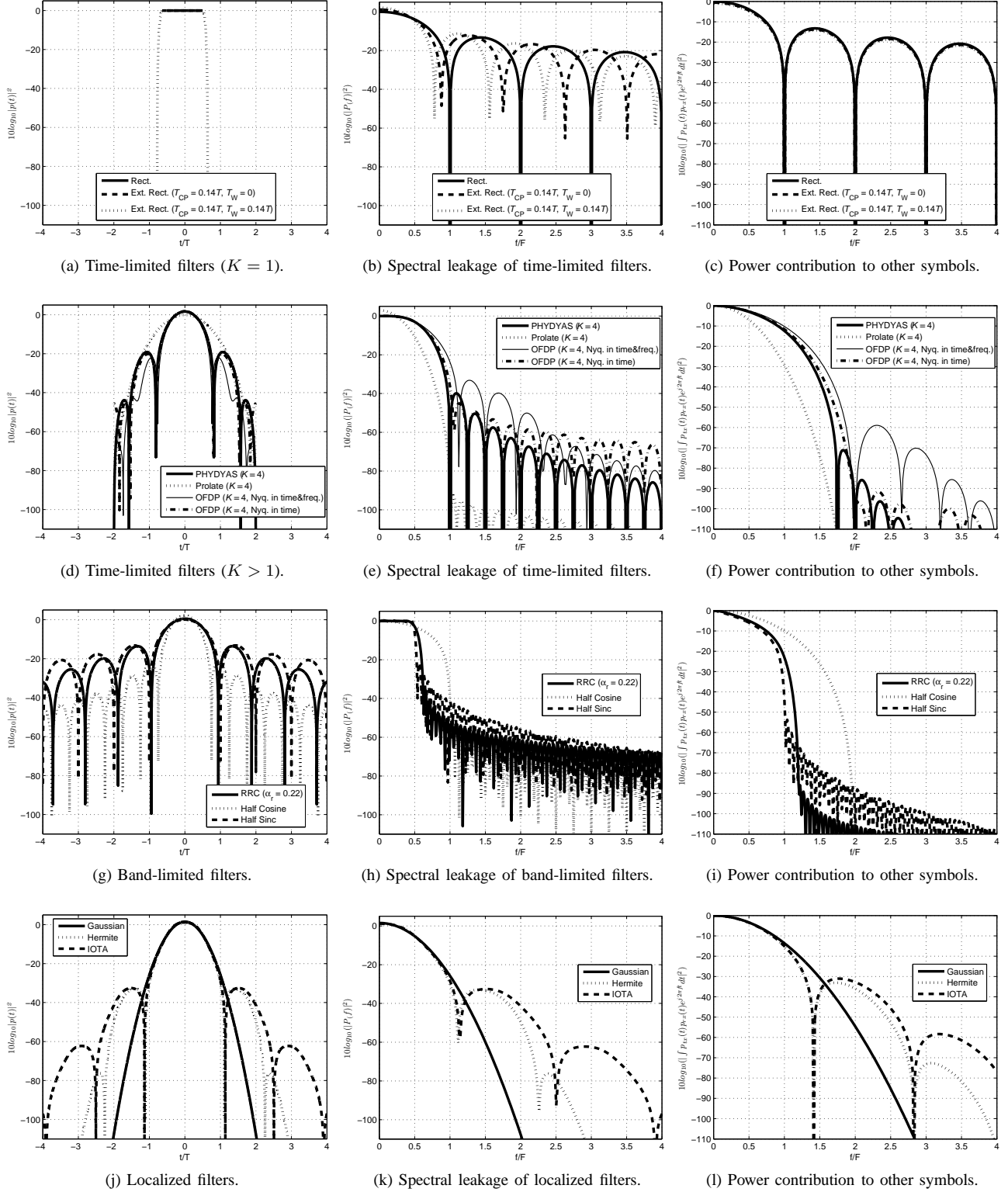
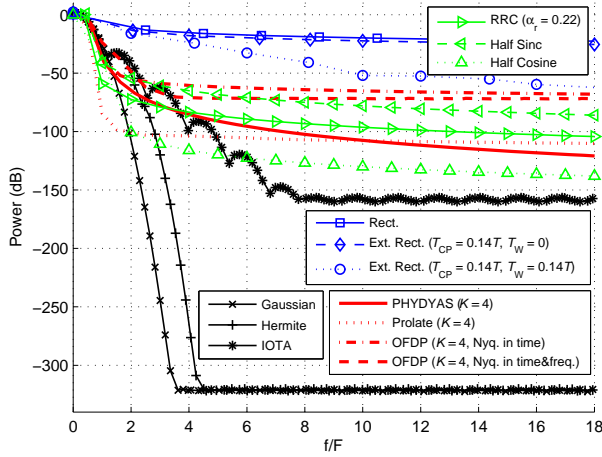


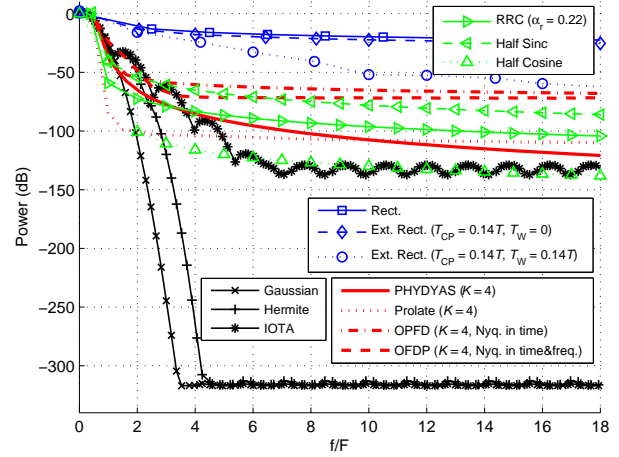
Fig. 6: Time and frequency characteristics of the filters and evaluating the filters in terms of Nyquist criterion in frequency domain.

for the less frequency dispersive channel scenarios as in Fig. 9 because it is more robust to time dispersion at the expense of CP overhead. Employing CP extends the null in ambiguity surface in time domain as given in Fig. 8(b).

However, FBMC approaches might be more robust to strong frequency dispersion depending on the filter used, such as Hermite, IOTA, OFDP, and PHYDYAS filters in Fig. 9(a), Fig. 9(c), and Fig. 9(d). Note that when CP is not used, OFDM



(a) 5 MHz bandwidth utilization.



(b) 20 MHz bandwidth utilization.

Fig. 7: Comparison of the power spectral densities of FBMC with different prototype functions considering LTE subcarriers utilization. Energy of each subcarrier is normalized to 1.

loses its advantages in multipath environments. Additionally, Fig. 9 shows that since OQAM allows more room for time-frequency spreading of prototype filters [12], OFDM/OQAM provides superior performance than OFDM/QAM when the same prototype filter is employed (e.g. rectangular/QAM versus rectangular/OQAM).

Time and frequency responses of the PHYDYAS, prolate, and OFDPs are given in Fig. 6(d). Since their durations are longer than the rectangular filter, they provide better spectral leakage performances compared to the rectangular filters as can be seen in Fig. 6(e). Especially, prolate filter provides very sharp decaying in frequency domain by discarding the Nyquist criterion. However, if the Nyquist criterion is provided, the out-of-band power is increasing as in OFDPs compared to the prolate filters. Also, providing the Nyquist criterion in both domains increases the sidelobes of the OFDPs. PHYDYAS filter provides very good out-of-band leakage characteristics. Note that Nyquist criterion in time does not hold when the time shift is more than 2 for PHYDYAS filter ($K = 4$) as given in Fig. 8(c). This issue yields better sidelobe performance compared to the OFDPs. Additionally, the out-of-band leakage performances of these filters in the system level are given in Fig. 7(a) and Fig. 7(b). They are also superior than conventional windowing approaches without degrading the spectral efficiency of the system.

The ambiguity surface of prolate filter given in Fig. 8(d) is similar to the ambiguity surface of the Gaussian pulse given in Fig. 8(j). However, it provides compact support for a given filter length in frequency domain instead of both time and frequency domains. Since OFDPs are derived from the proper combinations of prolate sequences, they are also compact in frequency domain while satisfying the Nyquist criterion. If the Nyquist criterion is provided only in time domain, OFDP gives minimal ICI contributions to the other symbols in frequency domain for a given filter length. Thus, exploiting OFDPs for FMT-based FBMC systems is more suitable compared to

RRC based filters, since there is no degradation on Nyquist criterion for OFDP because of the filter truncation. Indeed, if the Nyquist criterion is enforced in frequency domain, OFDP characteristics approach the rectangular pulse with longer filter length as shown in Fig. 8(f). Therefore one can interpret that OFDPs stays between RRC and rectangular pulse.

Both PHYDYAS filter and OFDPs have remarkably good SIR performances in Fig. 9 after Hermite and IOTA filters. Considering the SIR performances and their the finite durations, which corresponds to less complex systems, these filters are promising for FBMC based systems.

B. Band-limited Filters

As opposed to the time-limited, band-limited filters, i.e., RRC family given in Fig. 6(g), are ideally limited in frequency domain. However, in practical conditions, the power spectrum of these filters will deviate from ideal frequency localization as shown in Fig. 6(h) because of the filter truncation in time domain. While employing larger α_r (e.g., half cosine) results in larger bandwidth, using small α_r (e.g., half sinc) apparently increases the sidelobes of FBMC for the same filter length as given in Fig. 7(a) and Fig. 7(b). The impact of truncation can be clearly observable by using ambiguity surface for filters with small α_r factors. For example, half sinc does not satisfy the Nyquist criterion when $K = 16$ and the nulls for symbol spacing do not occur as in Fig. 8(i). In Fig. 10, the impact of the truncation is given in terms of SIR. Apparently, for lower α_r , the impact of truncation on SIR performance is highly dominant. For example, SIR is limited to 20.5 dB for $K = 16$ for half-sinc filter even if the channel dispersion is ignored. In [120], it is also mentioned that the orthogonality loss due to the shortly truncated RRC filters is compensated via equalization.

the frequency responses are almost flat in the passband region, which means that the per-subchannel equalizers also improved the frequency response of t

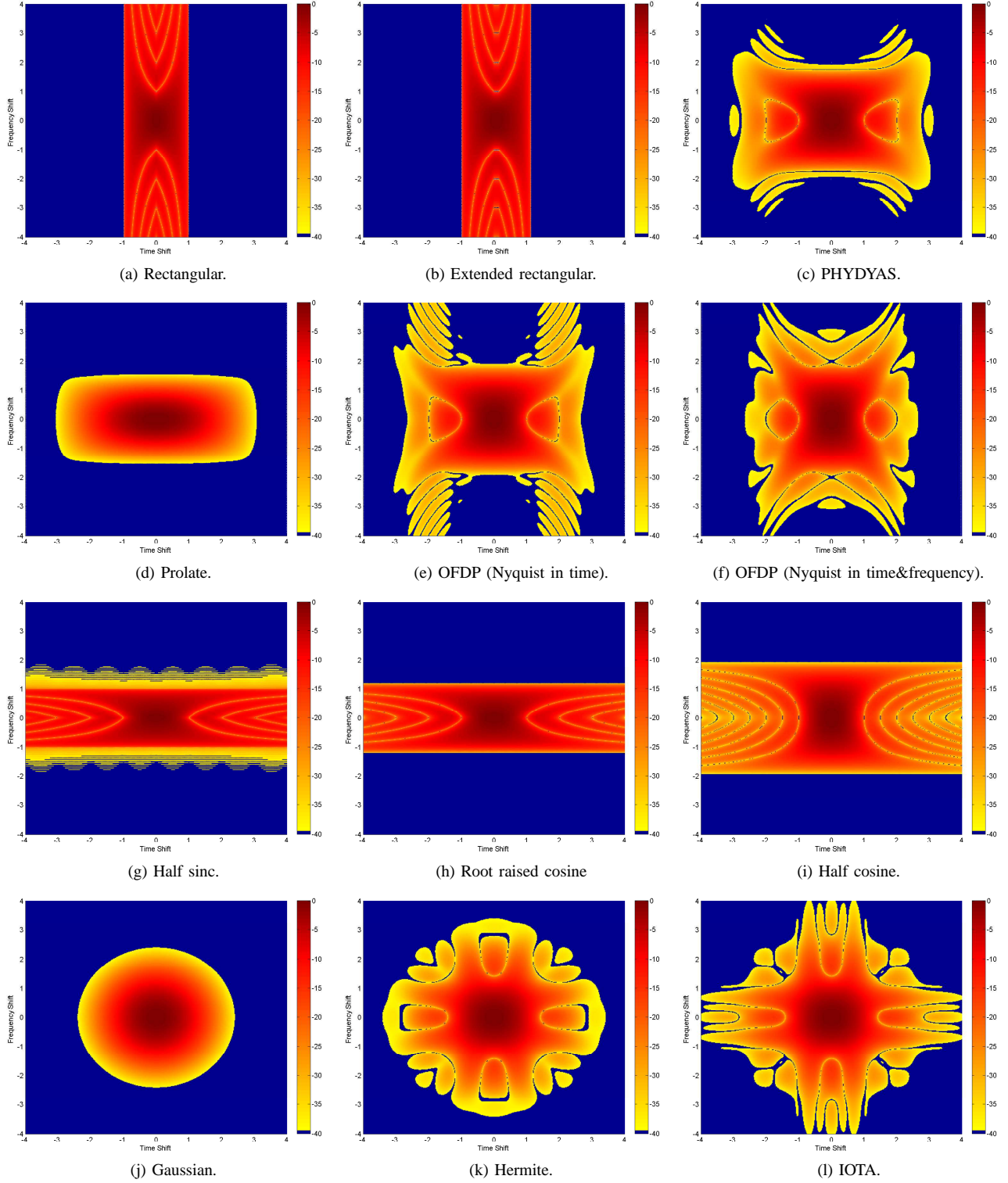


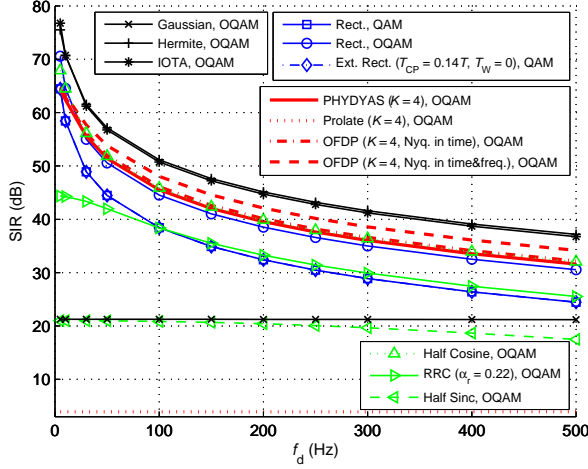
Fig. 8: Ambiguity surfaces of the well-known prototype filters in the literature ($10 \log_{10}(A(\phi, \psi))$).

In all plots in Fig. 9, half-cosine filter approaches to PHYDYAS and OFDP in terms of SIR performances since these filters are very similar to each other. However, decreasing α_r degrades the SIR performance of RRC, since the impact of the filter truncation on SIR becomes dominant due to the increasing sidelobes in time domain. Additionally, RRC and

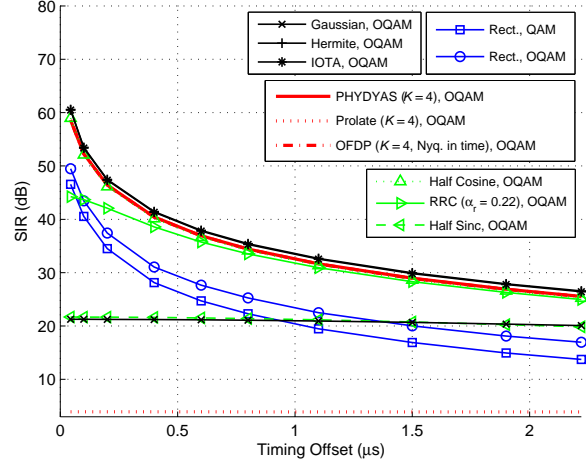
half-cosine filters approximately have the same immunity to timing misalignment as given in Fig. 9(b).

C. Localized Filters

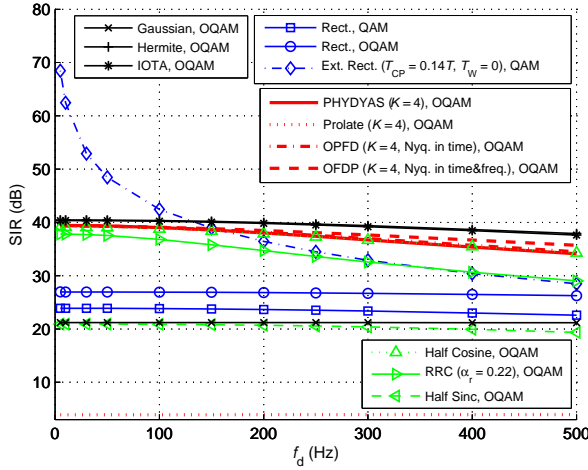
While time-limited and band-limited pulses have tendency to localize the energy in a single domain, localized filters



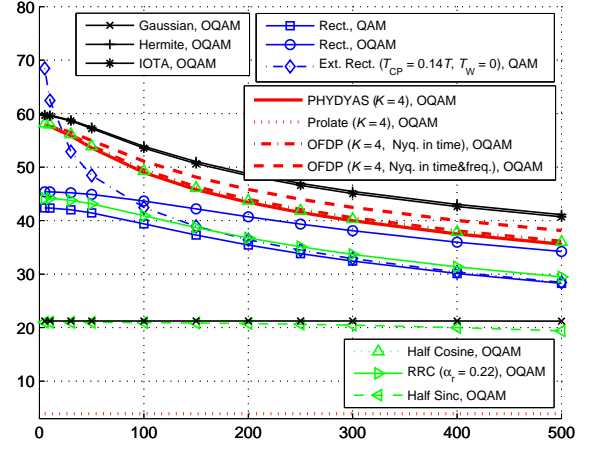
(a) Carrier Frequency Offset.



(b) Timing offset. Extended rectangular is not included since it satisfies the orthogonality in simulated timing offset range.



(c) ITU Vehicular A.



(d) ITU Pedestrian A.

Fig. 9: SIR performance of the prototype filters for different channel scattering functions

provide a compact support in both time and frequency domains. Therefore, the localized filters have isotropic responses in both time and frequency characteristics as in Fig. 6(j) and Fig. 6(k). The isotropic also corresponds to isotropic ambiguity surfaces as given in Fig. 8(j), Fig. 8(k), and Fig. 8(l). Gaussian filter provides a circular ambiguity surface without any nulls. However, the localization of Gaussian filter is the best compared to the other filters and decays fast in both time and frequency domain. Thus, in terms of out-of-band leakage, Gaussian filter yields better sidelobe performance as given in Fig. 7(a), and Fig. 7(b). In addition, the performance of the Gaussian filter is almost constant compared to the other filters as can be seen in Fig. 9. Even if Gaussian filter has worse SIR results, the required effort for equalization for FBMC with Gaussian filter might be less than other prototype filters since Gaussian pulse has the best time-frequency localization.

On the other hand, by slightly degrading the time-frequency localization performance of the Gaussian filter, Hermite and

IOTA achieve Nyquist criterion for $\tau_0 = \sqrt{2}T/2$ and $\nu_0 = \sqrt{2}F/2$ when $\alpha_g = 1$. Therefore, the nulls are located for every $\sqrt{2}F$ and $\sqrt{2}T$ as given in Fig. 6(l). In terms of out-of-band leakage, FBMC with Hermite filter provides superior frequency response compared to the IOTA filter as given in Fig. 7(a) and Fig. 7(b). When both SIR performance and out-of-power leakage are considered, Hermite and IOTA filters have the better characteristics because of two fundamental reasons: 1) very good joint time-frequency localization and 2) being orthogonal filters. Both of them provide very strong time-frequency dispersion immunity as well as CFO and timing misalignment robustness as given in Fig. 9(a) and Fig. 9(b). Additionally, the impact of filter truncations on SIR is not as dominant as other filters. For example, Hermite and IOTA filters with $K = 8$ is sufficient to yield more than 80 dB SIR as in Fig. 10. On the other hand, these filters lose their advantages for low Doppler scenarios compared with the extended rectangular, i.e. conventional OFDM. According to

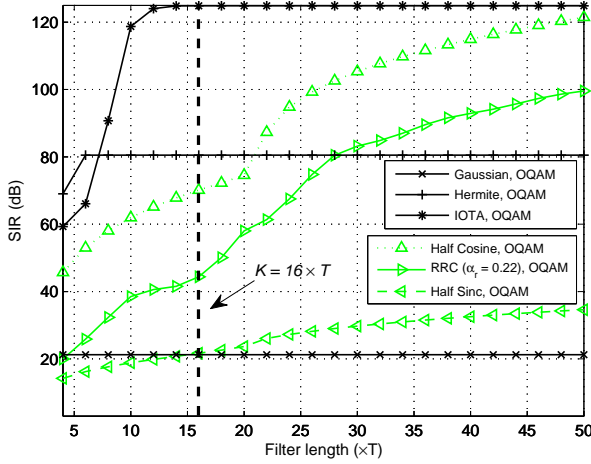


Fig. 10: Impact of filter truncation.

Fig. 9(c) and Fig. 9(d), while FBMC with Hermite and IOTA filters are better than conventional OFDM for $f_d > 135$ Hz for ITU Vehicular A, they provide better characteristics for frequencies as low as $f_d = 15$ Hz for ITU Pedestrian A.

VI. TRANSCEIVER DESIGN ISSUES

This section addresses several issues that have not been directly addressed in the earlier sections and that are related to implementation of FBMC systems. Representative references are provided to other related work in the literature and some of the key insights are highlighted. For a more comprehensive treatment and a larger body of literature related to these problems, readers are referred to corresponding references.

TABLE IV provides a classification of various references in the literature related to prototype filter design. This table should be treated as a set of representative references, and an attempt to tentatively capture and classify a large body of literature that are relevant to FBMC systems. In each column of TABLE IV, commonly used prototype filters in the FBMC literature are listed, while each row of the table includes a specific aspect of FBMC systems. References for different prior work on FBMC are placed in the table based on the prototype filters used in each reference, as well as the scope of the corresponding reference. The goal is to capture a tentative *research activity map* of this area, which is useful for understanding the key contributions and open research directions.

A. Lattice and Filter Adaptations

In a doubly-dispersive channel, the lattice and filter parameters that minimize ISI and ICI are given by [32], [54], [86]

$$\underbrace{\frac{\sigma_t}{\sigma_f} \propto \frac{\tau_{\text{rms}}}{f_{d,\text{max}}}}_{\text{pulse adaptation}}, \quad \underbrace{\frac{\tau_0}{\nu_0} \propto \frac{\tau_{\text{rms}}}{f_{d,\text{max}}}}_{\text{lattice adaptation}}, \quad (43)$$

where τ_{rms} is the root mean square (RMS) delay spread of the channel and f_d is the maximum Doppler shift. While

lattice adaptation corresponds to aligning τ_0 and ν_0 with τ_{rms} and $f_{d,\text{max}}$, *pulse adaptation* is equivalent to the dilation of the pulse depending on the channel dispersion in time and frequency. The rationale behind these adaptations are to match the proportion of the channel dispersion to the pulse dispersion in the time and frequency.

In an early study, [8], the pulse adaptation is given without theoretical explanations. In a later work, the identity of $\sigma_t/\sigma_f = \tau_{\text{max}}/f_{d,\text{max}}$ is obtained theoretically in [136] when $\tau_{\text{max}}f_{d,\text{max}} \rightarrow 0$. This identity is utilized in [16], [88] considering underspread channels and improved in [21], [32], [60], [86] considering the lattice adaptation. For example, in [21], both pulse adaptation and lattice adaptation are jointly optimized to adapt to the doubly-dispersive channel characteristics based on WSSUS assumption. Considering rectangular lattice and Gaussian filter, the optimum conditions for the pulse and lattice adaptations are derived as

$$S_H(\tau, \nu) = \delta(\tau)\delta(\nu) \Rightarrow \frac{\sigma_t}{\sigma_f} = \frac{\tau_{\text{max}}}{f_{d,\text{max}}} \quad (44)$$

$$S_H(\tau, \nu) = \frac{1}{2\tau_{\text{max}}f_{d,\text{max}}} \Rightarrow \frac{\sigma_t}{\sigma_f} = \frac{\tau_0}{\nu_0} = \frac{\tau_{\text{max}}}{f_{d,\text{max}}} \quad (45)$$

$$S_H(\tau, \nu) = \frac{e^{-\tau/\tau_{\text{rms}}} \times 1/\pi f_{d,\text{max}}}{\tau_{\text{rms}} \sqrt{1 - (\nu/f_{d,\text{max}})^2}} \Rightarrow \frac{\sigma_t}{\sigma_f} = \frac{\tau_0}{\nu_0} = \frac{1.5\tau_{\text{rms}}}{f_{d,\text{max}}} \quad (46)$$

where (45) corresponds to a doubly dispersive channel with a uniform delay power profile and uniform Doppler power spectrum, while (46) corresponds to a doubly dispersive channel with an exponential delay power profile and U-shape Doppler power spectrum.

In [32], a theoretical framework to adapt the pulse shape and lattice to varying channel conditions is introduced. It is emphasized that OFDM with a rectangular lattice is a suboptimal solution for doubly dispersive channels. Instead of rectangular symbol placement, if the lattice is constructed with a hexagonal shape, i.e. neighboring symbols located at each corner of hexagon, better protection against ISI and ICI compared to rectangular lattices is achieved since the minimum distance between symbols increases. For this purpose, a lattice generator matrix Λ is utilized to determine the frequency spacing and time spacing as

$$\begin{bmatrix} \text{Time spacing} \\ \text{Frequency spacing} \end{bmatrix} = \underbrace{\begin{bmatrix} \tau_0 & p\tau_0 \\ 0 & \nu_0 \end{bmatrix}}_{\Lambda} \begin{bmatrix} m \\ k \end{bmatrix} \quad (47)$$

where $p > 0$ [12]. While the choice of $p = 0$ yields rectangular lattice, $p = 0.5$ results in hexagonal structure. Note that both lattice structures provide the same spectral efficiency which is calculated by $\eta = \beta/\det\{\Lambda\}$. While the normalized minimum distance between symbols is 1 for rectangular lattice, it is obtained as $\sqrt{1.25}$ for hexagonal lattice. Therefore, the immunity of the system against time-frequency dispersion is increased without losing from the spectral efficiency. For exponential decaying and Jake's Doppler channel model, the improvement in signal-to-interference-plus-noise ratio (SINR) is in the range of 1-2 dB in case of forcing the Gaussian filter to be a Nyquist filter with maximum spectral efficiency. Additionally,

considering dilation and chirp operations, the pulse adaptation is combined with the hexagonal lattice structures. In [86], Lattice-OFDM is re-investigated with nonorthogonal pulses by emphasizing the fact that the orthogonalization procedure destroys the time-frequency concentration of the initial pulse. Instead of the maximizing number of symbols per second per hertz via the orthogonal pulses, orthogonality is abandoned with Weyl-Heisenberg frames similar to [21], and matching equations for the pulse and lattice adaptations are provided for the hexagonal lattice structure.

Note that it is not an easy task to develop a single lattice structure and a prototype filter for a system serving multiple users with different channel characteristics. To deal with the lattice and pulse design for such a system, while one might consider the worst case scenario to optimize pulse and lattice, other might include multiple lattices and filter structures within the frame. In [137], unlike the conventional orthogonal frequency division multiple accessing (OFDMA) frame structures that consider the worst case communication channel, multiple CP and subcarrier spacings are employed by taking the statistics of the mobility and the range of the users into account. As a result, better frequency spread immunity and higher spectral efficiency are obtained. Even if the proposed method does not apply pulse adaptation, intuitively, it offers lattice adaptation for multiple users.

B. Equalization

One of the features of FBMC transmission different from OFDM is the absence of CP. It is well-known that using CP longer than the maximum excess delay of the channel in OFDM allows single tap frequency domain equalization. FBMC follows a different rationale than OFDM by limiting the numbers of the symbols contributing to desired symbol in time and frequency domains and by exploiting good time-frequency localization properties of the filters. Hence, FBMC offers manageable ICI and ISI characteristics even in doubly dispersive channels, at the expense of relatively more complex equalization. Thus, considering the equalization complexity at the receiver is critically important for the sake of practical systems.

In [121] and [138], equalization methods for FBMC transmission are introduced under three categories. The first approach is to use well-localized prototype filters in order to deal with the time-frequency selectivity. The pulse energy is concentrated in time and frequency domains and the effects of ICI and ISI on the neighboring symbols are assumed to be limited. In this context, a basic single-tap subcarrier equalization per subcarrier might be employed to recover the symbols [64], [138], [139]. However, since single-tap equalizers use the inverse of the channel response at center frequency of each subcarrier, the performance of the channel estimation directly affects the equalization performance. The second (conventional) approach exploits fractional sampling to equalize the FBMC symbol via finite impulse response (FIR) filters. It is natural for the equalizer to work at the fractional sampling, e.g., $T/2$, since the FBMC symbols are generated with staggered modulations. In this category, it is

possible to develop equalizers considering different criteria. For example, minimum mean square error (MMSE) equalizers [123], [138], [140]–[142], maximum likelihood sequence estimator (MLSE) equalizer, [143], low-complexity equalizers [83], [121], [138], and channel tracking equalizers [95], [120], [144] all have different optimization goals. The third approach utilizes multiple taps via FIR filters for each subcarrier. The equalizer operates at the symbol rate and deals with the aliasing between the subcarriers for FBMC subcarriers that arise due to the staggered modulations [121]. Theoretically, it is possible to perform equalization at the symbol rate by exploiting equalizers which consider multiple subcarriers, but it does not bring any specific advantage compared to fractionally spaced equalizers [138].

C. MIMO

FBMC has been considered for wireless standards such as 3GPP in the past. However, one of the most critical challenges has been how to implement MIMO with FBMC, causing skepticism for further standardization studies. FMT, which is one of the FBMC variations as discussed in previous sections, can actually be conveniently used along with MIMO [59]. On the other hand, spectral efficiency of FMT is lower than that of OFDM/OQAM due to larger separation between the subchannels.

In [116], it was shown that MIMO with spatial multiplexing can be directly applied OFDM/OQAM when the MMSE equalization is utilized [114], [118]. Use of spatial multiplexing with maximum likelihood detection (MLD) or the Alamouti space time block coding (STBC) with FBMC remain to be challenging problems due to the signaling model of OFDM/OQAM [83], [114]. In particular, data is carried only by the real part of the signal in OFDM/OQAM, and imaginary part appears as an interference at the receiver [117], [118]. Therefore, MIMO techniques that are easy to implement in CP-OFDM such as STBC are no longer possible with OFDM/OQAM, and imaginary interference needs to be handled. While [115] proposes a method to cancel this imaginary interference for the case of single-delay space-time trellis coding (STTC) with two transmit and one receive antennas, [117] extends this to N_t transmit antennas and proposes an iterative decoding approach.

In [118], Alamouti coding was shown to be applicable to OFDM/OQAM when it is further combined with code division multiple access (CDMA). Recently, [114] introduced a new scheme referred as FFT-FBMC to remove the intrinsic interference, which yields a system model similar to OFDM. Hence, MIMO transmission schemes that are possible in OFDM, such as spatial multiplexing with MLD or Alamouti STBC, can also be utilized with FBMC. All in all, there still needs to be more studies on the application of MIMO to FBMC under practical implementation scenarios.

D. Cognitive Radio and Resource/Power Allocation

Due to its favorable properties, OFDM has been commonly considered as a candidate physical layer technology for dynamic spectrum access and cognitive radio systems [145]–[147]. FFT part of the OFDM demodulator can also be

conveniently utilized for spectrum sensing purposes to identify the presence of primary users in the vicinity [79], [148]. On the other hand, OFDM has its own drawbacks when used in cognitive radio applications. For example, sidelobes of the OFDM subcarriers may cause large interference leakage to neighboring channels. This prevents efficient utilization of unused portion of the spectrum by secondary users and hence limits the aggregate spectral efficiency of a cognitive radio system. Moreover, OFDM is highly sensitive to time/frequency synchronization errors, which puts stringent constraints for dynamic spectrum access in cognitive radio networks.

Low spectral leakage property of FBMC makes it an attractive candidate for cognitive radio systems [79]. While a subchannel in CMT or SMT overlaps with its immediate adjacent subchannels only, FMT variation of FBMC utilizes non-overlapping subchannels. As such, due to the minimization of spectral leakage to neighboring subchannels in FBMC, secondary users in a cognitive radio network may efficiently utilize the spectrum opportunities. Moreover, with FBMC, no tight synchronization is required between primary and secondary networks, which relaxes implementation complexity. Finally, [79] shows that the use of filter banks yields similar spectrum sensing accuracies when compared to those of optimum multi-taper based spectrum sensing [146], with less computational complexity.

Downlink resource allocation in FBMC-based cognitive radios is investigated in [77]. The goal is to maximize total capacity of the cognitive radio network, under certain constraints such as the total available power and interference threshold for primary users. Results show that an FBMC-based cognitive radio network yields higher aggregate spectral efficiency with significant gains under certain scenarios (up to 200% in some settings), and yields lower interference to the primary users.

In [101], uplink resource allocation in a multiple antenna cognitive radio system has been investigated. In this case, FBMC yields aggregate spectral efficiencies that are around 45% higher than those delivered by OFDM. A similar conclusion regarding uplink spectral efficiency has been reached in [106], while [72] shows through simulations that FBMC provides superior BERs when compared to OFDM in a multi-user uplink channel, at a much lower computational complexity. There are two main reasons for the spectral efficiency gain in both the downlink and the uplink when FBMC is used. Firstly, as opposed to OFDM, FBMC does not allocate any time (and hence, energy) to the transmission of a CP. Secondly, FBMC yields lower adjacent channel interference; this may improve the SINR of secondary users, and/or allow the use of smaller guard bands among subchannels.

In [40], a multi-mode uplink access method is proposed. In this approach, depending on the specific requirements of different users, different access methods such as SC-FDMA, FBMC, or FB-S-FBMC can be utilized by different users. Such a hybrid approach provides full flexibility in cognitive radio applications.

E. Time/Frequency Synchronization

Sensitivity of FBMC systems into time/frequency synchronization errors are investigated in [52] and [100] through

simulations, and in [90] through theoretical analysis. In [52] and [100], 2-D contour plots for which a given combination of CFO and fractional time delay (FTD) yields a 3 dB degradation in a target SINR are simulated for WiMAX systems. Results show that FBMC is less sensitive to CFOs compared to OFDM. On the other hand, in the presence of FTD, larger degradation observed in FBMC due to absence of a CP.

Handling combined effects of FTD and CFO in FBMC systems is a challenging problem, and requires advanced signal processing techniques in FBMC transceivers [90]. Theoretical analysis in [90] shows that FMT, at a cost of lower spectral efficiency when compared with SMT and CMT, is most robust against synchronization errors, especially at high SNR. For the uplink, FMT and OFDM/OQAM are particularly effective to combat against the degradation caused by the misalignments among the transmissions of different users (see also [60], [72]).

Time and frequency synchronization for FBMC systems have been addressed in [91], [92], [109]–[111]. Since there is no CP in FBMC, CP-based timing synchronization is not possible with FBMC as opposed to OFDM. While preamble-based, training-based, or blind synchronization methods as in OFDM are applicable, some modifications are required. In particular, presence of complementary interference from neighboring symbols (in time and frequency) necessitates the design of pilots that can work well with FBMC [109]. One approach that yields good performance is to use pilots and auxiliary pilots [108], [109], [124]. Alternatively, training sequence based [92] and non-data aided (blind) synchronization techniques are also available in the literature [149], [150].

F. Channel Estimation

As also mentioned, orthogonality of OFDM/OQAM holds only in the real field. Therefore, conventional channel estimation techniques for OFDM cannot be used without any modification for OFDM/OQAM, due to the *intrinsic* imaginary interference which is removed via $\Re\{\cdot\}$ operation [63], [104], [125], [138], [151]. To solve this problem, pilot-aided channel estimation techniques are proposed in [124]. In [63], an alternative preamble-based channel estimation approach named interference approximation method (IAM) by using real-valued symbols is introduced. It does not require a priori knowledge of the prototype function, and yields 1 dB gain in the BER performance when compared with CP-OFDM. In [104], the real-valued symbols are replaced with imaginary ones and 2 dB gain is achieved compared to CP-OFDM. Then, a general theoretical framework for IAM preamble design is given in [125]. Also, a comparative study on the preamble-based least square (LS) channel estimation is given for OQAM and QAM systems considering sparse preambles in [151].

G. 60 GHz Communications

Due to large bandwidths available, 60 GHz communications carries critical importance for next-generation broadband communication systems. Design of analog components is one of the important challenges at such high central frequencies, and may lead to radio-frequency (RF) front-end non-idealities such as phase noise (PN) and CFOs. OFDM, while coping well

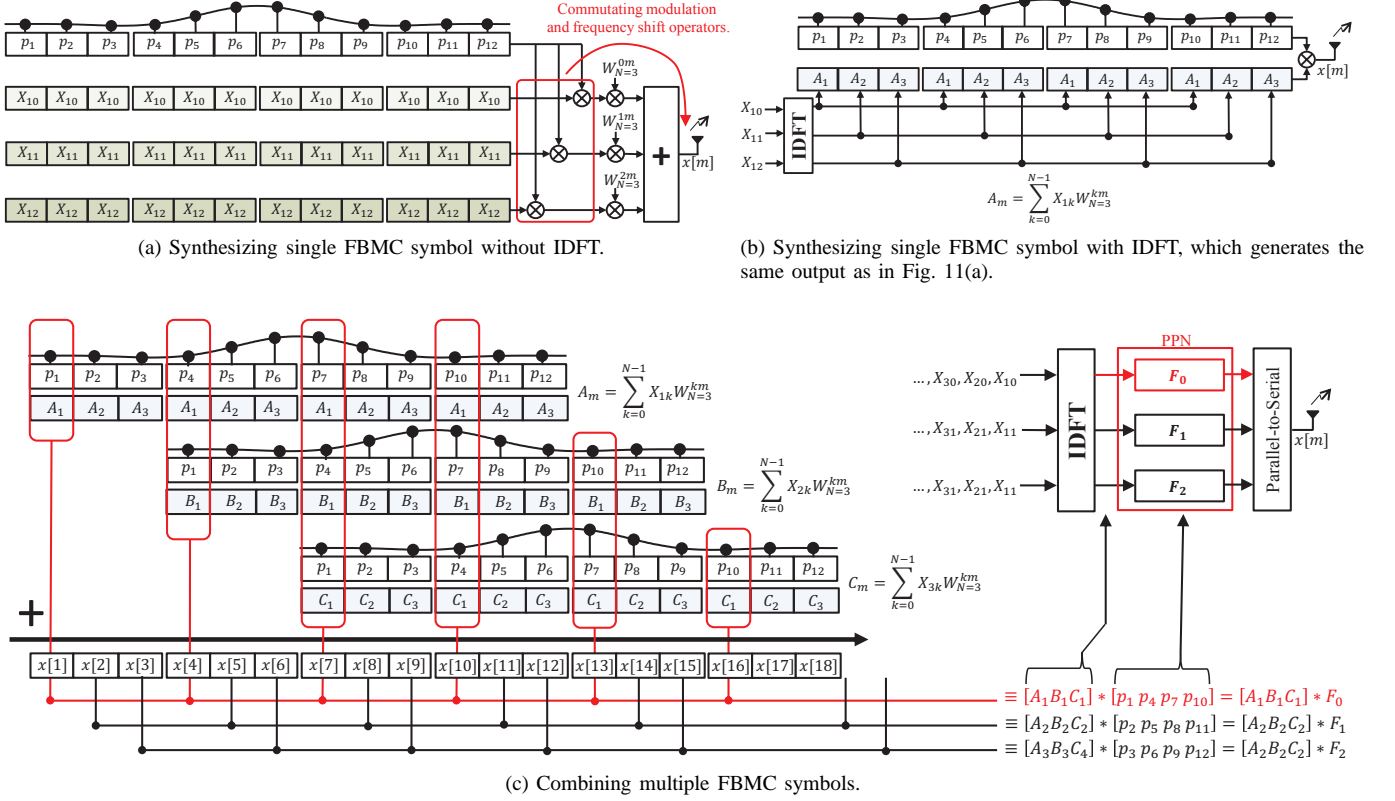


Fig. 11: Synthesizing FBMC symbols with IDFT operation. Note that X_{mk} is the information symbol on m th time slot and k th subcarrier, $[p_1, p_2, \dots, p_{KN}]$ are the samples of the prototype filter, and F_i are the polyphase components of the prototype filter.

with the high frequency selectivity that is typical for 60 GHz communications, is known to be very susceptible to PN and CFO. In [107], robustness of FBMC against the following non-idealities of 60 GHz communications are investigated and compared with continuous phase modulation (CPM): 1) high PN of the local oscillator at mixing stage, 2) low-power (and hence, low-resolution) requirement of analog-to-digital converter (ADC) due to high bit rates, and 3) distortion and spectral regrowth caused by non-linearities in the power amplifiers (PAs). While FBMC/OQAM has better spectral efficiency than CPM, results in [107] show that CPM is less sensitive to PN and ADC resolution imperfections, and allows more power efficient operation of the PA compared to FBMC.

H. Impact of Non-linear Power Amplifiers and PAPR Issues

The PAPR characteristics of OFDM and FBMC are compared in [40], [70], [78]. The PAPR of OFDM and FBMC are shown to be similar for various scenarios in [70], [78], with FBMC providing lower spectral sidelobes in its power spectral density. Similarly, [40] shows that FBMC and OFDM have practically identical PAPR cumulative distribution functions (CDFs). On the other hand, use of DFT-spreading [40], [66] and filter bank spreading [40] in conjunction with FBMC lowers the PAPR of the transmitted signals, yielding PAPRs that are close to those of SC-FDMA.

Impact of linear and non-linear PAs on the power spectral

densities (PSDs) of OFDM and FBMC are modeled and compared in [78]. While FBMC has significantly lower sidelobes than those of OFDM when the PA operates in the linear region, the benefit of FBMC diminishes when the PA operates in the non-linear region. Since the user equipments closer to the cell edge have to transmit with higher power levels due to power control. Therefore, they may have to operate in the non-linear region of the PAs and benefit of using FBMC might be incremental for such users.

I. Polyphase Implementation

FBMC introduces complexity by adding extra filters at the transmitter and the receiver. However, the complexity of FBMC can be reduced by exploiting polyphase representations of filters and FFT operations. As shown in Fig. 1, the polyphase network is after the FFT at the transmitter, and before the IFFT at the receiver, and they replace the CP insertion/removal blocks in OFDM. An illustrative scenario for analyzing and synthesizing FBMC symbols with 3 subcarriers are shown in Fig. 11 and Fig. 12, respectively, where both PPN and DFT implementations are described. It is assumed that the filter length is $4N$ where $N = 3$. Thus, the filter is effective for 12 samples for each FBMC symbol. First, single FBMC symbol is constructed in Fig. 11(a). After the prototype filter is multiplied with an information symbol in each branch, FBMC symbol is generated by combining the branches modulated

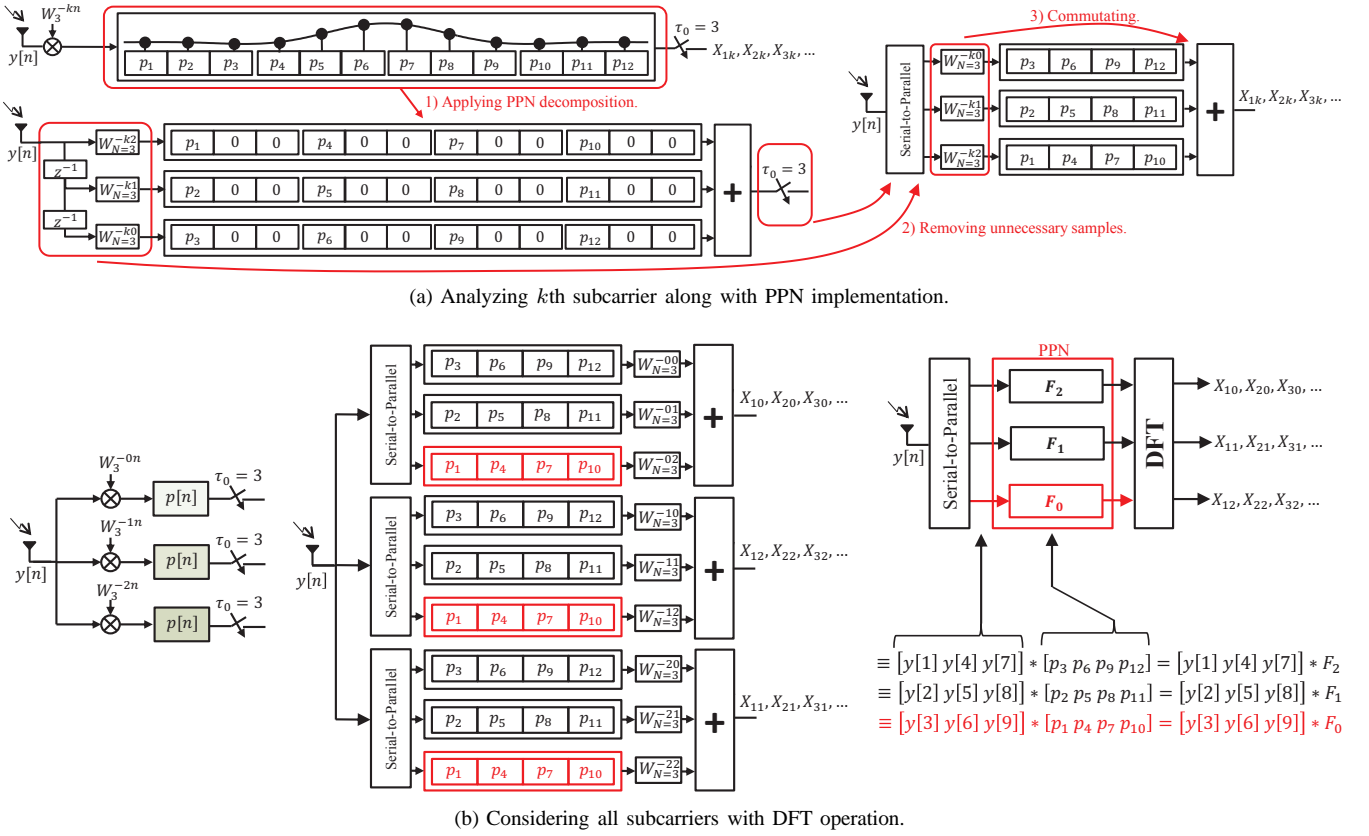


Fig. 12: Analyzing FBMC symbols with DFT operation.

via twiddle factors where $W_N^{mk} = e^{j2\pi mk/N}$. In Fig. 11(b), an equivalent diagram of Fig. 11(a) is realized with inverse discrete Fourier transformation (IDFT) operation by applying the multipliers indicated in Fig. 11(a) after the summation operation. To make these substitutions, the repetition of exponential term W_N^{nl} for every other three samples is exploited. In Fig. 11(c), three FBMC symbols are taken into consideration. Each FBMC symbol is shifted by symbol spacing, which is 3, and added to generate an FBMC frame. Indeed, this operation corresponds to a pattern as indicated in Fig. 11(c). In this example, operations involving all red boxes indicated on the figure correspond to PPN component F_0 . Essentially, the output of each IDFT result is filtered with some filter coefficients. Therefore, FBMC brings some additional filtering operations after IDFT operation. Note that these filters are simply equal to 1 for OFDM.

The basic idea behind the FBMC receiver consists of three basic steps; 1) Shifting the desired subcarrier to baseband. 2) Filtering the signal with receiving filter to eliminate the impacts of other subcarriers. 3) Sampling at correct instants. Considering these steps, analysis of a single subcarrier is given in Fig. 12(a). First, polyphase decomposition is applied to filter using shift operation (z^{-1}). Since the information symbols are constructed in every other 3 samples and the exponential term repeat itself around the unit circle, exponential terms can be distributed to each phase as factors. Also, since the intermediate samples are not necessary, the implementation is simplified using a commutator and removing the zero

coefficients at each branch. Then, by moving the positions of the exponential coefficients before summation operations and analyzing each subchannel, DFT operations is obtained as in Fig. 12(b). Similar to the transmitter, additional filtering operation is necessary before DFT operations.

The implementations given in Fig. 11 and Fig. 12 are suitable for non-staggered and staggered modulations. For staggered modulations, the structures have to be replicated for quadrature and in-phase part separately and combined with proper time shift to yield complete FBMC frames. In addition, DFT and IDFT operations should be centralized in time domain to implement even-symmetrical filters. Extended summaries on PPN are also provided in [7], [49], [152]. Additionally, PPN structure is implemented and discussed in [6], [42], [87], [88], [119], [153].

J. Testbeds and Extensions to Standards

While there are many publications theoretically comparing FBMC with OFDM and other waveforms, there are very limited number of works that discuss testbed implementation of FBMC are relatively limited. In [100], an FBMC testbed, which developed as a part of the PHYDYAS project [53], [154] is described. The testbed is capable of real-time transmission and reception of FBMC signals. Transmitter side involves a field-programmable gate array (FPGA) that includes the PHY layer only, and can operate both in OFDM and in FBMC modes. The receiver side is composed of an RF front-end, a USRP motherboard (involving ADCs and FPGA), and a

software subsystem.

Recently, there are also several studies that investigate the extension of FBMC technology into existing wireless standards. For example, FBMC has been considered in the context of WiMAX systems in [52], [100], [108], [154], and in the context of beyond 3G systems in [65], [66], [105]. Both [65] and [66] propose a modification in LTE frame structure so that it may be used together with FBMC. In particular, absence of a CP in FBMC enables the transmission of an additional OQAM symbol within one slot duration composed of seven complex OFDM symbols in LTE. While this extra OQAM symbol may also be utilized for other purposes, it has been used to improve the channel estimation quality in [65], [66]. In order to better assess the various implementation trade-offs between OFDM and FBMC, further studies are needed on the testbed experimentation.

K. Complexity Analysis

One of the important criteria for the adoption of FBMC in the future wireless standards is whether it can yield sufficiently better gains than existing techniques such as OFDM, at the cost of a reasonable complexity increase. The complexity of FBMC has been investigated in the literature from different perspectives in [5], [52], [68], [71], [72], [74], [81]–[83], [155]. As discussed in [52], the major factor for complexity increase in FBMC is due to the replacement of IFFT/FFT in OFDM with the filterbanks.

On the other hand, additional complexity has to be introduced into OFDM transmitter in order to suppress out-of-band power leakage, which is handled naturally by FBMC. A typical approach is to use active interference cancellation (AIC) in OFDM, which reserves a number of subcarriers at the edge of an OFDM band to suppress sidelobes in the PSD of OFDM [68], [71], [72]. Implementation of complex equalization and MIMO techniques in FBMC may also increase its complexity further, see e.g. [81], [83].

VII. CONCLUDING REMARKS AND DISCUSSION

Waveform design is one of critical issues for future radio access technologies. Recently, filter bank based multicarrier schemes, re-emerging as an umbrella for the conventionally employed schemes, stand as an exciting and promising concept. In this study, the waveform design issues are examined under the filter bank based multicarrier transmission and reception techniques. Starting with Gabor systems, a framework on the prototype filter design is provided considering both orthogonality and biorthogonality properties. We emphasize that while having lower lattice density provides better SIR performance in doubly dispersive channels, SIR performance can be maximized with the optimum biorthogonal filters by extending the concept of orthogonality to biorthogonality. In addition, conventional FBMC approaches, i.e., SMT and CMT, provide high equalization complexity. Therefore, the impact of biorthogonal filters to the equalization domain is described. Many Gabor systems consider the design of optimum filters that maximize the SIR performance. In this paper, we further emphasize the need for Gabor systems which also consider the

receiver equalization complexity to combat with the doubly dispersive channel characteristics.

In this study, the various performances of the well-known prototype filters in literature are investigated considering different tools and metrics. According to the results, even if OFDM benefits from CP utilization yielding simple frequency domain equalization for low Doppler spreads, it loses its advantage for higher frequency dispersion. Hermite and IOTA filters achieves higher SIR for the environments with higher frequency dispersion, and intrinsically provide better sidelobe characteristics. On the other hand, PHYDYAS filter and OFDP achieve superior SIR performances with finite durations which allow less complex structures at the receiver and transmitters. Also, compared to the other prototype filters, RRC with higher α_r , Hermite, and IOTA filters are robust to the filter truncation.

It is important to emphasize that filters introduce different characteristics and trade-offs to the schemes. Therefore, it is not an easy task to develop a single Gabor system that addresses every aspects of the systems. With the current technologies, three main aspect cannot be ignored in the design of the accessing schemes: simplification of the equalization, MIMO functionality, and applicability to the network. OFDM addresses the simplification of the equalizers and MIMO functionality with the exploitation of CP. However, efficient utilization of OFDM is still a discussion considering heterogeneous and denser networks. The heterogeneous and denser networks are the promising wireless approaches, since they allow systems to operate at the same spectra. Recently, significant efforts have been devoted to maximize the spectral efficiency and network throughput within novel networking strategies. At that point, FBMC approaches provide a perspective to examine the schemes in terms of filter that also includes these networking scenarios. Beside these facts, exploiting other degree of freedoms such as having multiple users in the system can be considered as another open research area.

ACKNOWLEDGMENT

This study has been supported by DOCOMO Innovations, Inc.

REFERENCES

- [1] R. W. Chang, "Synthesis of band-limited orthogonal signals for multichannel data transmission," *The Bell System Technical J.*, pp. 1775–1796, Dec. 1966.
- [2] B. Saltzberg, "Performance of an efficient parallel data transmission system," *IEEE Trans. Commun. Technol.*, vol. 15, no. 6, pp. 805–811, Dec. 1967.
- [3] S. Weinstein and P. Ebert, "Data transmission by frequency-division multiplexing using the discrete fourier transform," *IEEE Trans. Commun. Technol.*, vol. 19, no. 5, pp. 628–634, Oct. 1971.
- [4] A. Peled and A. Ruiz, "Frequency domain data transmission using reduced computational complexity algorithms," in *Proc. IEEE Int. Conf. Acoustics, Speech, Sig. Proc. (ICASSP)*, vol. 5, Apr. 1980, pp. 964–967.
- [5] B. Hirosaki, "An orthogonally multiplexed QAM system using the discrete Fourier transform," *IEEE Trans. Commun.*, vol. 29, no. 7, pp. 982–989, Jul. 1981.
- [6] M. Bellanger, G. Bonnerot, and M. Coudreuse, "Digital filtering by polyphase network: Application to sample-rate alteration and filter banks," *IEEE Trans. Acoustics, Speech and Sig. Proc.*, vol. 24, no. 2, pp. 109–114, Apr. 1976.

- [7] P. Vaidyanathan, "Multirate digital filters, filter banks, polyphase networks, and applications: A tutorial," *Proc. of the IEEE*, vol. 78, no. 1, pp. 56–93, Jan. 1990.
- [8] B. Le Floch, M. Alard, and C. Berrou, "Coded orthogonal frequency division multiplex," *Proceedings of the IEEE*, vol. 83, no. 6, pp. 982–996, Jun. 1995.
- [9] P. Siohan, C. Siclet, and N. Lacaille, "Analysis and design of OFDM/OQAM systems based on filterbank theory," *IEEE Trans. Sig. Proc.*, vol. 50, no. 5, pp. 1170–1183, May 2002.
- [10] M. Bellanger, "Specification and design of a prototype filter for filter bank based multicarrier transmission," in *Proc. IEEE Int. Conf. Acoustics, Speech, Sig. Proc. (ICASSP)*, vol. 4, Salt Lake City, UT, May 2001, pp. 2417–2420.
- [11] B. Farhang-Boroujeny, "OFDM versus filter bank multicarrier," *IEEE Sig. Proc. Mag.*, vol. 28, no. 3, pp. 92–112, May 2011.
- [12] J. Du and S. Signell, "Classic OFDM systems and pulse-shaping OFDM/OQAM systems," *Technical Report (KTH - Royal Institute of Technology)*, pp. 1–32, Feb. 2007.
- [13] F. Hlawatsch and G. Matz, *Wireless Communications Over Rapidly Time-Varying Channels*, ser. Academic Press. Elsevier Science, 2011.
- [14] P. Jung and G. Wunder, "The WSSUS pulse design problem in multicarrier transmission," *IEEE Trans. Commun.*, vol. 55, no. 10, pp. 1918–1928, Sep. 2007.
- [15] Cisco, "Global mobile data traffic forecast update, 20112016," pp. 1–29, Feb. 2012, white Paper.
- [16] W. Kozek and A. Molisch, "Nonorthogonal pulseshapes for multicarrier communications in doubly dispersive channels," *IEEE J. Select. Areas Commun. (JSAC)*, vol. 16, no. 8, pp. 1579–1589, Oct. 1998.
- [17] I. Trigui, M. Siala, S. Affes, A. Stéphenne, and H. Boujemâa, "Optimum pulse shaping for OFDM/BFDM systems operating in time varying multi-path channels," in *Proc. IEEE Global Telecommun. Conf. (GLOBECOM)*, Washington, D.C., Nov. 2007, pp. 3817–3821.
- [18] P. L. Sondergaard, "Finite discrete Gabor analysis," Ph.D. dissertation, Danmarks Tekniske Universitet, 2007.
- [19] H. Bolcskei, P. Duhamel, and R. Heiss, "Design of pulse shaping OFDM/OQAM systems for high data-rate transmission over wireless channels," in *Proc. IEEE Int. Conf. Commun. (ICC)*, vol. 1, Vancouver, Canada, June 1999, pp. 559–564.
- [20] R. Haas and J. Belfiore, "A time-frequency well-localized pulse for multiple carrier transmission," *Wireless Personal Commun.*, vol. 5, no. 1, pp. 1–18, July 1997.
- [21] F. M. Han and X. Zhang, "Wireless multicarrier digital transmission via Weyl-Heisenberg frames over time-frequency dispersive channels," *IEEE Trans. Commun.*, vol. 57, no. 6, pp. 1721–1733, June 2009.
- [22] W. Kozek, H. Feichtinger, and T. Strohmer, "Time-frequency synthesis of statistically matched Weyl-Heisenberg prototype signals," in *Proc. IEEE International Symposium on Signal Processing (SP)*, Oct. 1994, pp. 21–24.
- [23] R. J. Duffin and A. C. Schaeffer, "A class of nonharmonic fourier series," *Transactions of the American Mathematical Society*, vol. 72, no. 2, pp. 341–366, Mar. 1952.
- [24] O. Christensen, *An Introduction to Frames and Riesz Bases*, ser. Applied and Numerical Harmonic Analysis. Birkhäuser, 2003.
- [25] G. Strang and T. Nguyen, *Wavelets and Filter Banks*. Wellesley-Cambridge Press, 1996.
- [26] I. Daubechies, "The wavelet transform, time-frequency localization and signal analysis," *IEEE Trans. Inf. Theory*, vol. 36, no. 5, pp. 961–1005, Sep. 1990.
- [27] J. E. Mazo, "Faster-Than-Nyquist Signaling," *The Bell System Technical J.*, vol. 54, pp. 1451–1462, Oct. 1975.
- [28] A. Liveris and C. Georgiades, "Exploiting faster-than-Nyquist signaling," *IEEE Trans. Commun.*, vol. 51, no. 9, pp. 1502–1511, Sep. 2003.
- [29] F. Rusek and J. Anderson, "The two dimensional Mazo limit," in *Proc. IEEE Int. Symp. on Information Theory (ISIT)*, Sep. 2005, pp. 970–974.
- [30] F. Rusek and J. B. Anderson, "Successive interference cancellation in multistream faster-than-Nyquist signaling," in *Proc. Intl. Wireless Comm. and Mobile Computing Conf.* New York, NY, USA: ACM, 2006, pp. 1021–1026.
- [31] P. Kabal and S. Pasupathy, "Partial-response signaling," *IEEE Trans. Commun.*, vol. 23, no. 9, pp. 921–934, Sep. 1975.
- [32] T. Strohmer and S. Beaver, "Optimal OFDM design for time-frequency dispersive channels," *IEEE Trans. Commun.*, vol. 51, no. 7, pp. 1111–1122, Jul. 2003.
- [33] G. Cherubini, E. Eleftheriou, and S. Olcer, "Filtered multitone modulation for very high-speed digital subscriber lines," *IEEE J. Select. Areas Commun.*, vol. 20, no. 5, pp. 1016–1028, June 2002.
- [34] —, "Filtered multitone modulation for VDSL," in *Proc. IEEE Global Telecommun. Conf. (GLOBECOM)*, vol. 2, Rio de Janeiro, Brazil, Dec. 1999, pp. 1139–1144.
- [35] H. Sari, G. Karam, and I. Jeanclaude, "Frequency-domain equalization of mobile radio and terrestrial broadcast channels," in *Proc. IEEE Global Telecommun. Conf. (GLOBECOM)*, vol. 1, Dec. 1994, pp. 1–5.
- [36] H. Sari, G. Karam, and I. Jeanclaude, "Transmission techniques for digital terrestrial tv broadcasting," *Communications Magazine, IEEE*, vol. 33, no. 2, pp. 100–109, Feb. 1995.
- [37] D. Falconer, S. Ariyavisitakul, A. Benyamin-Seeyar, and B. Eidson, "Frequency domain equalization for single-carrier broadband wireless systems," *Communications Magazine, IEEE*, vol. 40, no. 4, pp. 58–66, Apr. 2002.
- [38] H. G. Myung, J. Lim, and D. J. Goodman, "Single carrier FDMA for uplink wireless transmission," *Vehicular Technology Magazine, IEEE*, vol. 1, no. 3, pp. 30–38, Sep. 2006.
- [39] G. Berardinelli, L. Ruiz de Temino, S. Frattasi, M. Rahman, and P. Mogensen, "OFDMA vs. SC-FDMA: performance comparison in local area IMT-A scenarios," *Wireless Communications, IEEE*, vol. 15, no. 5, pp. 64–72, Oct. 2008.
- [40] T. Ihalainen, A. Viholainen, T. Stitz, M. Renfors, and M. Bellanger, "Filter bank based multi-mode multiple access scheme for wireless uplink," in *Proc. European Signal Processing Conf. (EUSIPCO)*, vol. 9, Glasgow, Scotland, Aug. 2009, pp. 1354–1358.
- [41] T. Weiss, J. Hillenbrand, A. Krohn, and F. Jondral, "Mutual interference in OFDM-based spectrum pooling systems," in *Proc. IEEE Vehic. Technol. Conf. (VTC)*, vol. 4, May. 2004, pp. 1873–1877.
- [42] W. Rhee, J. Chuang, and L. Cimini Jr, "Performance comparison of OFDM and multitone with polyphase filter bank for wireless communications," in *Proc. IEEE Veh. Technol. Conf. (VTC)*, vol. 2, Ottawa, Canada, May 1998, pp. 768–772.
- [43] A. Viholainen, "Prototype filter and structure optimization," Jan. 2009, PHYDYAS Project Document.
- [44] A. Vahlin and N. Holte, "Optimal finite duration pulses for OFDM," *IEEE Trans. Commun.*, vol. 44, no. 1, pp. 10–14, Jan. 1996.
- [45] P. Halpern, "Optimum finite duration Nyquist signals," *IEEE Trans. Commun.*, vol. 27, no. 6, pp. 884–888, Jun. 1979.
- [46] G. Nigam, R. Singh, and A. Chaturvedi, "Finite duration root nyquist pulses with maximum in-band fractional energy," *IEEE Commun. Lett.*, vol. 14, no. 9, pp. 797–799, Sep. 2010.
- [47] J. Kaiser and R. Schafer, "On the use of the 10-sinh window for spectrum analysis," *IEEE Trans. Acoust., Speech, Signal Proc.*, vol. 28, no. 1, pp. 105–107, Feb. 1980.
- [48] F. F. Kuo and J. Kaiser, *System Analysis by Digital Computer (Chapter 7)*. New York: Wiley, 1966.
- [49] B. Farhang-Boroujeny, *Signal processing techniques for software radios*. Lulu, 2008.
- [50] K. W. Martin, "Small side-lobe filter design for multitone data-communication applications," *IEEE Trans. Circuits and Systems-II: Analog and Digital Signal Processing*, vol. 45, no. 8, pp. 1155–1161, Aug. 1998.
- [51] M. Bellanger, "FBMC physical layer: A primer," *PHYDYAS FP7 Project Document*, Jan. 2010.
- [52] F. Schaich, "Filterbank based multi carrier transmission (FBMC) evolving OFDM: FBMC in the context of WiMAX," in *Proc. European Wireless Conf. (EW)*, Lucca, Italy, Apr. 2010, pp. 1051–1058.
- [53] B. Farhang-Boroujeny and C. Yuen, "Cosine modulated and offset QAM filter bank multicarrier techniques: a continuous-time prospect," *EURASIP J. Advances in Sig. Proc.*, vol. Dec., pp. 1–6, 2010.
- [54] J. Du and S. Signell, "Pulse shape adaptivity in OFDM/OQAM systems," in *Proc. Int. Conf. Advanced Infocomm Technology (ICAIT)*, Shen Zhen, China, July 2008.
- [55] A. Tonello, "Performance limits for filtered multitone modulation in fading channels," *IEEE Trans. Wireless Commun.*, vol. 4, no. 5, pp. 2121–2135, Sep. 2005.
- [56] P. Schniter, "On the design of non-(bi) orthogonal pulse-shaped FDM for doubly-dispersive channels," in *Proc. Int. Conf. Acoustics, Speech, and Sig. Proc. (ICASSP)*, vol. 3, Montreal, Canada, May 2004, pp. 817–820.
- [57] T. Kurt, M. Siala, and A. Yongacoglu, "Multi-carrier signal shaping employing Hermite functions," in *Proc. European Sig. Proc. Conf. (EUSIPCO)*, Antalya, Turkey, Sep. 2005.
- [58] S. Aldirmaz, A. Serbes, and L. Durak-Ata, "Spectrally efficient OFDMA lattice structure via toroidal waveforms on the time-frequency plane," *EURASIP J. Advances in Sig. Proc.*, pp. 1–13, June 2010.

- [59] P. Amini, C. Yuen, R. Chen, and B. Farhang-Boroujeny, "Isotropic filter design for MIMO filter bank multicarrier communications," in *Proc. IEEE Sensor Array and Multichannel Sig. Proc. Workshop (SAM)*, Israel, Oct. 2010, pp. 89–92.
- [60] J. Du, "Pulse shape adaptation and channel estimation in generalised frequency division multiplexing," Stockholm, Sweden, Dec. 2008.
- [61] P. Siohan and C. Roche, "Cosine-modulated filterbanks based on extended Gaussian functions," *IEEE Trans. Sig. Proc.*, vol. 48, no. 11, pp. 3052–3061, Nov. 2000.
- [62] J. Du and S. Signell, "Time frequency localization of pulse shaping filters in OFDM/OQAM systems," in *Proc. Int. Conf. Information, Commun., and Sig. Proc.*, Singapore, Dec. 2007, pp. 1–5.
- [63] C. L   , J. Javaudin, R. Legouable, A. Skrzypczak, and P. Siohan, "Channel estimation methods for preamble-based OFDM/OQAM modulations," *European Trans. Telecommun.*, vol. 19, no. 7, pp. 741–750, Nov. 2008.
- [64] C. L   , P. Siohan, R. Legouable, and J. Javaudin, "Preamble-based channel estimation techniques for OFDM/OQAM over the powerline," in *Proc. IEEE Int. Symp. Power Line Communications and Its Applications (ISPLC)*, Pisa, Italy, Mar. 2007, pp. 59–64.
- [65] M. Gharba, R. Legouable, and P. Siohan, "An alternative multiple access scheme for the uplink 3GPP/LTE based on OFDM/OQAM," in *Proc. IEEE Int. Symp. Wireless Commun. Syst. (ISWCS)*, York, England, Sep. 2010, pp. 941–945.
- [66] M. Gharba, H. Lin, P. Siohan, and F. Labeau, "DFT-OQAMA: an alternative multiple access for future mobile networks," in *Proc. IEEE Veh. Technol. Conf.*, Quebec City, Canada, Sep. 2012.
- [67] M. Bellanger, "Physical layer for future broadband radio systems," in *Proc. IEEE Radio and Wireless Symp. (RWS)*, Jan. 2010, pp. 436–439.
- [68] W. Jiang and M. Schellmann, "Suppressing the out-of-band power radiation in multi-carrier systems: A comparative study," in *Proc. IEEE Global Telecommun. Conf. (GLOBECOM)*, Anaheim, CA, Dec. 2012.
- [69] W. Kozek, G. Pfander, J. Ungermann, and G. Zimmermann, "A comparison of various MCM schemes," in *Proc. Int. OFDM Workshop*, Hamburg, Germany, Sep. 2000, pp. 201–204.
- [70] D. Waldhauser, L. Baltar, and J. Nossek, "Comparison of filter bank based multicarrier systems with OFDM," in *Proc. IEEE Asia Pacific Conf. on Circuits and Systems (APCCAS)*, Singapore, Dec. 2006, pp. 976–979.
- [71] L. Baltar, D. Waldhauser, and J. Nossek, "Out-of-band radiation in multicarrier systems: a comparison," *Springer Lecture notes in Electrical Engineering*, vol. 1, pp. 107–116, 2007.
- [72] H. Saeedi-Sourck, Y. Wu, J. Bergmans, S. Sadri, and B. Farhang-Boroujeny, "Complexity and performance comparison of filter bank multicarrier and OFDM in uplink of multicarrier multiple access networks," *IEEE Trans. Sig. Proc.*, vol. 59, no. 4, pp. 1907–1912, 2011.
- [73] J. Du and S. Signell, "Comparison of CP-OFDM and OFDM/OQAM in doubly dispersive channels," in *Proc. Future Generation Communication and Networking (FGCN)*, vol. 2, Jeju-Island, Korea, Dec. 2007, pp. 207–211.
- [74] Q. Zhang, A. Kokkeler, and G. Smit, "An oversampled filter bank multicarrier system for cognitive radio," in *Proc. IEEE Int. Symp. Personal, Indoor and Mobile Radio Commun. (PIMRC)*, Cannes, France, Sep. 2008, pp. 1–5.
- [75] W. Xiang, J. Russell, and Y. Wang, "ICI reduction through shaped OFDM in coded MIMO-OFDM systems," *Int. J. Advances in Telecommun.*, vol. 3, no. 3 and 4, pp. 194–205, May 2011.
- [76] B. Farhang-Boroujeny, "A square-root Nyquist (M) filter design for digital communication systems," *IEEE Trans. Sig. Proc.*, vol. 56, no. 5, pp. 2127–2132, May 2008.
- [77] M. Shaat and F. Bader, "Computationally efficient power allocation algorithm in multicarrier-based cognitive radio networks: OFDM and FBMC systems," *EURASIP J. Advances in Sig. Proc.*, vol. 2009, pp. 1–13, Dec. 2010.
- [78] Z. Kollar and P. Horvath, "Physical layer considerations for cognitive radio: Modulation techniques," in *Proc. IEEE Veh. Technol. Conf. (VTC)*, Budapest, Hungary, May 2011, pp. 1–5.
- [79] B. Farhang-Boroujeny and R. Kempter, "Multicarrier communication techniques for spectrum sensing and communication in cognitive radios," *IEEE Commun. Mag.*, vol. 46, no. 4, pp. 80–85, Apr. 2008.
- [80] F. Dovis, M. Mondin, and F. Daneshgaran, "The modified Gaussian: a novel wavelet with low sidelobes with applications to digital communications," *IEEE Commun. Lett.*, vol. 2, no. 8, pp. 208–210, 1998.
- [81] N. Benvenuto, S. Tomasin, and L. Tomba, "Equalization methods in OFDM and FMT systems for broadband wireless communications," *IEEE Trans. Commun.*, vol. 50, no. 9, pp. 1413–1418, 2002.
- [82] M. Bellanger, "Filter banks and OFDM-OQAM for high throughput wireless LAN," in *Proc. Int. Symp. Commun., Control, and Sig. Proc. (ISCCSP)*, St. Julian's, Malta, Mar. 2008, pp. 758–761.
- [83] T. Ihalainen, A. Ikhlef, J. Louveaux, and M. Renfors, "Channel equalization for multi-antenna FBMC/OQAM receivers," *IEEE Trans. Veh. Technol.*, vol. 60, no. 5, pp. 2070–2085, June 2011.
- [84] N. J. Baas and D. P. Taylor, "Pulse shaping for wireless communication over time- or frequency-selective channels," *IEEE Trans. Commun.*, vol. 52, no. 9, pp. 1477–1479, Sep. 2004.
- [85] P. Jung and G. Wunder, "Iterative pulse shaping for Gabor signaling in WSSUS channels," in *Proc. IEEE Workshop on Sig. Proc. Advances in Wireless Commun. (SPAWC)*, Lisbon, Portugal, July 2004, pp. 368–372.
- [86] F.-M. Han and X.-D. Zhang, "Hexagonal multicarrier modulation: A robust transmission scheme for time-frequency dispersive channels," *IEEE Trans. Sig. Proc.*, vol. 55, no. 5, pp. 1955–1961, May 2007.
- [87] D. Schafhuber, G. Matz, and F. Hlawatsch, "Pulse-shaping OFDM/BFDM systems for time-varying channels: ISI/ICI analysis, optimal pulse design, and efficient implementation," in *Proc. IEEE Int. Symp. Personal, Indoor and Mobile Radio Commun. (PIMRC)*, vol. 3, Lisboa, Portugal, Sep. 2002, pp. 1012–1016.
- [88] G. Matz, D. Schafhuber, K. Grochenig, M. Hartmann, and F. Hlawatsch, "Analysis, optimization, and implementation of low-interference wireless multicarrier systems," *IEEE Trans. Wireless Commun.*, vol. 6, no. 5, pp. 1921–1931, May 2007.
- [89] R. Vitenberg, "Effect of carrier frequency offset and phase noise on the performance of WFMT systems," in *Int. Symp. Commun. Inform. Technol. (ISCIT)*, Bangkok, Thailand, 2006, pp. 633–637.
- [90] T. Fusco, A. Petrella, and M. Tanda, "Sensitivity of multi-user filter-bank multicarrier systems to synchronization errors," in *Proc. IEEE Int. Symp. Commun., Control, Sig. Proc. (ISCCSP)*, St. Julian's, Malta, Mar. 2008, pp. 393–398.
- [91] A. Petrella, "Synchronization algorithms for FBMC systems," *Ph.D. Dissertation*, 2009.
- [92] T. Fusco, A. Petrella, and M. Tanda, "Data-aided symbol timing and CFO synchronization for filter bank multicarrier systems," *IEEE Trans. Wireless Commun.*, vol. 8, no. 5, pp. 2705–2715, May 2009.
- [93] A. Tonello and S. Pupolin, "Discrete multi-tone and filtered multi-tone architectures for broadband asynchronous multi-user communications," in *Proc. Wireless Personal Multimedia Commun. (WPMC) Symp.*, Aalborg, Denmark, Sep. 2001, pp. 9–12.
- [94] R. Vitenberg, "A wavelet based filtered multi-tone," in *Proc. Int. Conf. Advanced Commun. Technol. (ICACT)*, vol. 3, Phoenix Park, Korea, Feb. 2008, pp. 1849–1853.
- [95] I. Berenguer and I. Wassell, "Efficient FMT equalization in outdoor broadband wireless systems," in *Proc. IEEE Int. Symp. Advances in Wireless Commun.*, Victoria, Canada, Sep. 2002.
- [96] A. Tonello and R. Vitenberg, "An efficient wavelet based filtered multitone modulation scheme," in *Proc. Wireless Personal Multimedia Commun. Symp. (WPMC)*, Abano Terme, Sep. 2004, pp. 436–439.
- [97] Q. Bai and J. Nossek, "On the effects of carrier frequency offset on cyclic prefix based OFDM and filter bank based multicarrier systems," in *Proc. IEEE Sig. Proc. Adv. Wireless Commun. (SPAWC)*, Marrakech, Morocco, June 2010, pp. 1–5.
- [98] I. Estella, A. Pascual-Iserte, and M. Payaro, "OFDM and FBMC performance comparison for multistream MIMO systems," in *Future Network and Mobile Summit*, Florence, Italy, June 2010, pp. 1–8.
- [99] Y. Medjahdi, M. Terre, D. L. Ruyet, D. Roviras, and A. Dziri, "Performance analysis in the downlink of asynchronous OFDM/FBMC based multi-cellular networks," *IEEE Trans. Wireless Commun.*, vol. 10, no. 8, pp. 2630–2639, Aug. 2011.
- [100] V. Ringset, H. Rustad, F. Schaich, J. Vandermot, and M. Najjar, "Performance of a filterbank multicarrier (FBMC) physical layer in the WiMAX context," in *Proc. Future Network and Mobile Summit*, Florence, Italy, June 2010, pp. 1–8.
- [101] M. Payar  , A. Pascual-Iserte, A. Garcia-Armada, and M. S  nchez-Fern  ndez, "Resource allocation in multi-antenna MAC networks: FBMC vs OFDM," in *Proc. IEEE Veh. Technol. Conf. (VTC)*, Budapest, Hungary, May 2011, pp. 1–5.
- [102] Y. Medjahdi, M. Terr  , D. Ruyet, and D. Roviras, "A new model for interference analysis in asynchronous multi-carrier transmission," *Arxiv Preprint – 1006.4278*, June 2010.
- [103] D. Lacroix, N. Goudard, and M. Alard, "OFDM with guard interval versus OFDM/OffsetQAM for high data rate UMTS downlink transmission," in *IEEE Veh. Technol. Conf. (VTC)*, vol. 4, Atlantic City, NJ, Oct. 2001, pp. 2682–2686.

- [104] C. L   , P. Siohan, R. Legouable, and R. Legouable, "2 dB better than CP-OFDM with OFDM/OQAM for preamble-based channel estimation," in *Proc. IEEE Int. Conf. Commun. (ICC)*, Beijing, China, Jun. 2008, pp. 1302–1306.
- [105] T. Ihalainen, T. Stitz, A. Viholainen, and M. Renfors, "Performance comparison of LDPC-coded FBMC and CP-OFDM in beyond 3G context," in *Proc. IEEE Int. Symp. Circuits and Systems*, Island of Kos, Greece, May 2006, pp. 1–4.
- [106] H. Zhang, D. Le Ruyet, D. Roviras, Y. Medjahdi, and H. Sun, "Spectral efficiency comparison of OFDM/FBMC for uplink cognitive radio networks," *EURASIP J. Advances in Sig. Proc.*, pp. 1–14, Dec. 2009.
- [107] J. Nsenga, W. Van Thillo, F. Horlin, A. Bourdoux, and R. Lauwereins, "Comparison of OQPSK and CPM for communications at 60 GHz with a nonideal front end," *EURASIP J. Wireless Commun. Networking*, vol. 2007, no. 1, pp. 51–51, 2007.
- [108] T. Stitz, A. Viholainen, T. Ihalainen, and M. Renfors, "CFO estimation and correction in a WiMAX-like FBMC system," in *Proc. IEEE Workshop on Sig. Proc. Adv. in Wireless Commun. (SPAWC)*, Perugia, Jun. 2009, pp. 633–637.
- [109] T. Stitz, T. Ihalainen, A. Viholainen, and M. Renfors, "Pilot-based synchronization and equalization in filter bank multicarrier communications," *EURASIP J. Advances in Sig. Proc.*, pp. 1–9, Dec. 2009.
- [110] T. Fusco, A. Petrella, and M. Tanda, "Joint symbol timing and CFO estimation for OFDM/OQAM systems in multipath channels," *EURASIP J. Advances in Sig. Proc.*, vol. Dec., pp. 1–11, 2009.
- [111] T. Stitz, T. Ihalainen, and M. Renfors, "Practical issues in frequency domain synchronization for filter bank based multicarrier transmission," in *Proc. IEEE Int. Symp. Commun. Control and Sig. Proc. (ISCCSP)*, St. Julians, Malta, Mar. 2008, pp. 411–416.
- [112] M. Payar  , A. Pascual-Iserte, and M. N  jar, "Performance comparison between FBMC and OFDM in MIMO systems under channel uncertainty," in *Proc. European Wireless Conf. (EW)*, Lucca, Apr. 2010, pp. 1023–1030.
- [113] R. Zakaria, D. Le Ruyet, and M. Bellanger, "Maximum likelihood detection in spatial multiplexing with FBMC," in *Proc. European Wireless Conference (EW)*, Lucca, Apr. 2010, pp. 1038–1041.
- [114] R. Zakaria and D. Le Ruyet, "A novel filter-bank multicarrier scheme to mitigate the intrinsic interference: Application to MIMO systems," *IEEE Trans. Wireless Commun.*, vol. 11, no. 3, pp. 1112–1123, Mar. 2012.
- [115] M. Bellanger, "Transmit diversity in multicarrier transmission using OQAM modulation," in *Proc. IEEE Int. Symp. Wireless Pervasive Computing (ISWPC)*, May 2008, pp. 727–730.
- [116] M. E. Tabach, J.-P. Javadin, and M. Helard, "Spatial data multiplexing over OFDM/OQAM modulations," in *Proc. IEEE Int. Conf. Commun. (ICC)*, Glasgow, Scotland, June 2007, pp. 4201–4206.
- [117] C. L    and D. L. Ruyet, "Decoding schemes for FBMC with single-delay STTC," *EURASIP J. Adv. in Sig. Proc.*, pp. 1–11, Dec. 2010.
- [118] C. L   , P. Siohan, and R. Legouable, "The alamouti scheme with CDMA-OFDM/OQAM," *EURASIP J. Adv. in Sig. Proc.*, pp. 1–13, Dec. 2010.
- [119] C. Lee and K. Yoo, "Polyphase filter-based OFDM transmission system," in *Proc. IEEE Veh. Technol. Conf. (VTC)*, vol. 1, Milan, Italy, May 2004, pp. 525–528.
- [120] D. Waldhauser, L. Baltar, and J. Nossek, "Adaptive equalization for filter bank based multicarrier systems," in *Proc. IEEE International Symposium on Circuits and Systems (ISCAS)*, May 2008, pp. 3098–3101.
- [121] T. Ihalainen, T. H. Stitz, M. Rinne, and M. Renfors, "Channel equalization in filter bank based multicarrier modulation for wireless communications," *EURASIP J. Appl. Signal Process.*, vol. 2007, no. 1, pp. 140–157, Jan. 2007.
- [122] R. Datta, G. Fettweis, Z. Kollar, and P. Horvath, "FBMC and GFDM interference cancellation schemes for flexible digital radio PHY design," in *Proc. Euromicro Conf. Digital System Design (DSD)*, Oulu, Finland, Sept. 2011, pp. 335–339.
- [123] A. Ikhlef and J. Louveaux, "An enhanced MMSE per subchannel equalizer for highly frequency selective channels for FBMC/OQAM systems," in *Proc. IEEE Workshop on Sig. Proc. Advances in Wireless Commun. (SPAWC)*, Perugia, Italy, June 2009, pp. 186–190.
- [124] J.-P. Javadin, D. Lacroix, and A. Rouxel, "Pilot-aided channel estimation for OFDM/OQAM," in *Proc. IEEE Vehic. Technol. Conf. (VTC)*, vol. 3, Jeju, Korea, Apr. 2003, pp. 1581–1585.
- [125] J. Du and S. Signell, "Novel preamble-based channel estimation for OFDM/OQAM systems," in *Proc. IEEE Int. Conf. Commun. (ICC)*, Jun. 2009, pp. 1–6.
- [126] H. Lin and P. Siohan, "Robust channel estimation for OFDM/OQAM," *IEEE Commun. Lett.*, vol. 13, no. 10, pp. 724–726, Oct. 2009.
- [127] H. Zhang, D. Le Ruyet, D. Roviras, and H. Sun, "Non-cooperative multi-cell resource allocation of FBMC based cognitive radio systems," *IEEE Trans. Veh. Technol.*, vol. 61, no. 2, pp. 799–811, Feb. 2012.
- [128] P. Amini, R. Kempter, R. Chen, L. Lin, and B. Farhang-Boroujeny, "Filter bank multitone: A physical layer candidate for cognitive radios," in *Proc. Software Defined Radio Technical Conference (SDR)*, Irvine, CA, Nov. 2005, pp. 14–18.
- [129] E. Azarnasab, R. Kempter, N. Patwari, and B. Farhang-Boroujeny, "Filterbank multicarrier and multicarrier CDMA for cognitive radio systems," in *Proc. IEEE Int. Conf. Cognitive Radio Oriented Wireless Networks and Commun. (CROWNCOM)*, Orlando, FL, Aug. 2007, pp. 472–481.
- [130] P. Bello, "Characterization of randomly time-variant linear channels," *IEEE Trans. Commun. Syst.*, vol. 11, no. 4, pp. 360–393, Dec. 1963.
- [131] G. Matz, "Statistical characterization of non-WSSUS mobile radio channels," *e& i Elektrotechnik und Informationstechnik*, vol. 122, no. 3, pp. 80–84, Mar. 2005.
- [132] W. Kozek and A. Molisch, "On the eigenstructure of underspread WSSUS channels," in *Proc. IEEE Workshop on Sig. Proc. Advances in Wireless Commun. (SPAWC)*, Apr. 1997.
- [133] T. Rappaport, *Wireless Communications: Principles and Practice*, 2nd ed. Upper Saddle River, NJ, USA: Prentice Hall PTR, 2001.
- [134] ITU Recommendation, "ITU-R M.1225 Guidelines for Evaluation of Radio Transmission Technologies for IMT-2000," in , 1997, p. 2450.
- [135] T. Feng and T. R. Field, "Statistical analysis of mobile radio reception: An extension of Clarke's model," *IEEE Trans. Commun.*, vol. 56, no. 12, pp. 2007–2012, Dec. 2008.
- [136] H. Feichtinger and T. Strohmer, *Gabor Analysis and Algorithms: Theory and Applications*, ser. Applied and Numerical Harmonic Analysis. Birkh  user, 1998.
- [137] A. Sahin and H. Arslan, "Multi-user aware frame structure for OFDMA based system," in *Proc. IEEE Veh. Technol. Conf. (VTC)*, Quebec City, Canada, Sep. 2012, pp. 1–5.
- [138] PHYDYAS, "Equalization and demodulation in the receiver (single antenna)," Deliverable D3.1, July 2008.
- [139] B. Farhang-Boroujeny, "Multicarrier modulation with blind detection capability using cosine modulated filter banks," *IEEE Trans. Commun.*, vol. 51, no. 12, pp. 2057–2070, Dec. 2003.
- [140] B. Hirosaki, "An analysis of automatic equalizers for orthogonally multiplexed QAM systems," *IEEE Trans. Commun.*, vol. 28, no. 1, pp. 73–83, Jan. 1980.
- [141] D. Waldhauser, L. Baltar, and J. Nossek, "MMSE subcarrier equalization for filter bank based multicarrier systems," in *Proc. IEEE Workshop on Sig. Proc. Advances in Wireless Commun. (SPAWC)*, Jul. 2008, pp. 525–529.
- [142] N. Holte, "MMSE equalization of OFDM/OQAM systems for channels with time and frequency dispersion," in *Proc. IEEE International Conference on Wireless Communications Signal Processing (WCSP)*, Nov. 2009, pp. 1–5.
- [143] L. Baltar, A. Mezghani, and J. Nossek, "MLSE and MMSE subchannel equalization for filter bank based multicarrier systems: Coded and uncoded results," in *Proc. European Signal Processing Conference (EUSIPCO)*, Aalborg, Denmark, Aug. 2010.
- [144] D. Waldhauser, L. Baltar, and J. Nossek, "Adaptive decision feedback equalization for filter bank based multicarrier systems," in *Proc. IEEE International Symposium on Circuits and Systems (ISCAS)*, May 2009, pp. 2794–2797.
- [145] G. Bansal, M. Hossain, and V. Bhargava, "Optimal and suboptimal power allocation schemes for OFDM-based cognitive radio systems," *IEEE Trans. Wireless Commun.*, vol. 7, no. 11, pp. 4710–4718, Nov. 2008.
- [146] S. Haykin, "Cognitive radio: brain-empowered wireless communications," *IEEE J. Select. Areas Commun.*, vol. 23, no. 2, pp. 201–220, Feb. 2005.
- [147] I. F. Akyildiz, W.-Y. Lee, M. C. Vuran, and S. Mohanty, "NeXt generation/dynamic spectrum access/cognitive radio wireless networks: A survey," *Elsevier Computer Networks*, vol. 50, no. 13, pp. 2127–2159, Sept. 2006.
- [148] T. Yucek and H. Arslan, "A survey of spectrum sensing algorithms for cognitive radio applications," *IEEE Commun. Surveys and Tutorials*, vol. 11, no. 1, pp. 116–130, Jan. 2009.
- [149] T. Fusco, A. Petrella, and M. Tanda, "Blind carrier frequency offset estimation for non-critically sampled FMT systems in multipath channels," in *IEEE Workshop on Sig. Proc. Adv. Wireless Commun. (SPAWC)*, Helsinki, Finland, June 2007, pp. 1–5.

- [150] T. Fusco and M. Tanda, "Blind frequency-offset estimation for OFDM/OQAM systems," *IEEE Trans. Sig. Proc.*, vol. 55, no. 5, pp. 1828–1838, May 2007.
- [151] D. Katselis, E. Kofidis, A. Rontogiannis, and S. Theodoridis, "Preamble-based channel estimation for CP-OFDM and OFDM/OQAM systems: A comparative study," *IEEE Trans. Sig. Proc.*, vol. 58, no. 5, pp. 2911–2916, May 2010.
- [152] P. Vaidyanathan, "Multirate systems and filter banks, 1993."
- [153] M. Bellanger and J. Daguet, "TDM-FDM transmultiplexer: Digital polyphase and FFT," *IEEE Trans. Commun.*, vol. 22, no. 9, pp. 1199–1205, Sep. 1974.
- [154] PHYDYAS, "WiMAX simulation results, lab setup, and measurements," Deliverable D9.2, July 2009.
- [155] S. Mehmood, D. Dasalukunte, and V. Owall, "Hardware architecture of IOTA pulse shaping filters for multicarrier systems," *IEEE Trans. Circuits and Systems I: Regular Papers*, vol. PP, no. 99, p. 1, 2012.

TABLE IV: Classification of papers related to FBMC.

	RRC	PHYDYAS	Gaussian	Hermite	PSWF	IOTA	EGF	Half Cos.	Other
Surveys and Basic Principles	[2], [11]	[8], [43], [51], [67], [68]	[8], [12]	[53]	[11]	[8], [11], [12], [53], [69]		[11], [53]	[11], [12], [43], [53]
PSD Comparison	[9], [11], [33], [70]–[76]	[10], [68], [76]–[78]	[57]	[20], [57], [59]	[9], [11], [44], [79]	[11], [19], [57], [59]	[9], [73]	[11], [73]	[11], [19], [33], [57], [73], [75], [80]
Complexity Analysis	[71], [74], [81]	[52], [68], [82]							[5], [72], [83]
Pulse Design for Doubly Dispersive and WSSUS Channels	[11], [73], [84]		[14], [21], [54], [55], [85], [86]	[16], [17], [20], [53], [59]	[11]	[11], [14], [32], [53], [59], [85]	[54], [73]	[11], [53], [54], [73]	[11], [14], [16], [32], [53], [55], [73], [85], [87], [88]
Time/Frequency Localization Analysis	[9], [11], [73]		[12], [54], [73]	[16], [17], [20]	[9], [11]	[8], [11], [12], [32], [61], [62]	[9], [54], [61], [62], [73]	[8], [54], [62], [73]	[8], [12], [16], [32], [62], [73], [89]
CMT				[53]		[53]		[53]	[53]
FMT	[33], [34], [81], [90]–[92]		[55], [93]						[33], [42], [55], [59], [89], [93]–[96]
OFDM vs FBMC Comparison	[33], [70], [71], [73], [74], [81], [97]	[43], [52], [77], [98]–[102]	[12], [55], [93]	[17], [59]		[12], [40], [59], [103], [104]	[73]	[73]	[12], [33], [42], [43], [55], [65], [72], [73], [73], [87], [88], [93], [104], [105]
Uplink Performance	[90], [40]	[106]							[72]
RF Impairments (PA issues, etc.)	[107]	[43]							[43]
PAPR Performance	[40], [70], [76], [84]	[43], [76], [78]							[43]
Time/Frequency Synchronization and Robustness	[73], [76], [90]–[92], [97]	[52], [76], [99], [100], [102], [108]–[110]	[54], [56]			[73]	[54], [73]	[54], [73]	[56], [72], [73], [89], [111]
MIMO	[75]	[98], [112]–[115]	[59]			[114], [116]–[118]			[59], [75], [83]
Polyphase Implementation	[9]	[43]					[9]		[5], [9], [42], [43], [72], [119]
Equalization	[33], [81], [107], [120]–[122]	[82], [109], [123]							[33], [83], [95], [105], [111]
Channel Estimation						[63], [64], [104], [124]	[125]		[64], [104], [111], [126]
Biorthogonal FBMC			[56]	[16], [17]					[16], [56], [87], [88]
LTE/WiMAX Implementation		[100], [108], [109]							[65], [66]
Cognitive Radio	[74]	[43], [77], [78], [106], [127]			[79], [128]				[43], [129]
Resource/Power Allocation		[77], [101], [106], [127]	[93]						[93]
60 GHz Communications	[107]								
DFT and Filterbank Spreading	[40]	[43]							[43]
New Lattice Structure			[86]	[58]		[32]			[32]
Testbed		[100]							[94], [96]

